ENVISAT GOMOS Monthly report: December 2003

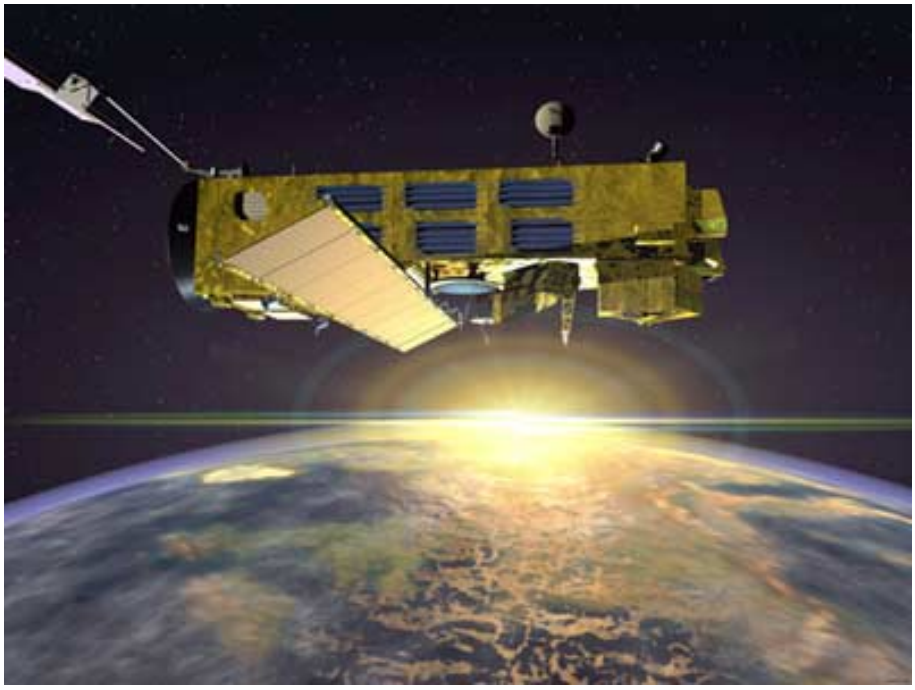

Prepared by:	PCF Team	ESA EOP-GOQ
Inputs from:	GOMOS Quality Working Group	
Issue:	1.0	
Reference:	ENVI-SPPA-EOPG-TN-04-0004	
Date of issue:	02 February 2004	
Status:	Reviewed	
Document type:	Technical Note	
Approved by:	Pascal Lecomte, Rob Koopman	

TABLE OF CONTENTS

1 INTRODUCTION

1.1 Scope

The main objective of the Monthly Report is to give, on a regular basis, the status of GOMOS instrument performance, data acquisition, results of anomaly investigations, calibration activities and validation campaigns. The following six sections compose the MR:

1 Summary
2 Unavailability
3 Instrument Performance and Configuration
4 Level 1 Product Quality Monitoring
5 Level 2 Product Quality Monitoring
6 Validation Activities and Results

In addition, the group interfaces with the Atmospheric Chemistry Validation Team.

1.2 References

[1] ENVISAT Weekly Mission Operations Report #80, #81, #82 ENVI-ESOC-OPS-RP-1011-TOS-OF
[2] 'Level 1b Detailed Processing Model', PO-RS-ACR-GS-0001, issue 5.4, 20 Nov, 2002
[3] 'Level 2 Detailed Processing Model', PO-RS-ACR-GS-0002, issue 5.4, 20 Nov, 2002
[4] Fortuin, P.J. and Kelder, H., ozone climatology based on ozone sonde and satellite measurements, J. Geophys. Res. 103, 31709-31734, 1998.

1.3 Acronyms and Abbreviations

ACVT	Atmospheric Chemistry Validation Team
ADF	Auxiliary Data File
ADS	Auxiliary Data Server
ANX	Ascending Node Crossing
ARF	Archiving Facility (PDS)
CCU	Central Communication Unit
CFS	CCU Flight Software
CNES	Centre National d'Études Spatiales
CTI	Configuration Table Interface / Configurable Transfer Item
CR	Cyclic Report
DC	Dark Charge
DMOP	Detailed Mission Operation Plan
DPM	Detailed Processing Model
DS	Data Server
DSA	Dark Sky Area
DSD	Data Set Descriptor

ECMWF	European Centre for Medium Weather Forecast
EQSOL	Equipment Switch Off Line
ESA	European Space Agency
ESL	Expert Support Laboratory
ESRIN	European Space Research Institute
ESTEC	European Space Research & Technology Centre
ESOC	European Space Operations Centre
FCM	Fine Control Mode
FMI	Finnish Meteorological Institute
FOCC	Flight Operations Control Centre (ENVISAT)
FP1	Fast Photometer 1
FP2	Fast Photometer 2
GADS	Global Annotations Data Set
GOMOS	Global Ozone Monitoring by Occultation of Stars
GOPR	GOmos PRototype
GS	Ground Segment
HK	Housekeeping
IASB	Institut d'Aeronomie Spatiale de Belgique
IAT	Interactive Analysis Tool
ICU	Instrument Control Unit
IDL	Interactive Data Language
IECF	Instrument Engineering and Calibration Facilities
IMK	Institute of Meteorology Karlsruhe (Meteorologisch Institut Karlsuhe)
INV	Inventory Facilities (PDS)
IPF	Instrument Processing Facilities (PDS)
JPL	Jet Propulsion Laboratory
LAN	Local Area Network
LPCE	Laboratoire de Physique et Chimie de l'Environnement
LUT	Look Up Table
MCMD	Macro Command
MDE	Mechanism Drive Electronics
MIP	Most Illuminated Pixel
MPH	Main Product Header
MPS	Mission Planning System
MR	Monthly Report
OBT	On Board Time
OCM	Orbit Control Manoeuvre
OOP	Out-of-plane
OP	Operational Phase of ENVISAT
PAC	Processing and Archiving Centre (PDS)
PCF	Product Control Facility
PDCC	Payload Data Control Centre (PDS)
PDHS	Payload Data Handling Station (PDS)
PDHS-E	Payload Data Handling Station – ESRIN
PDHS-K	Payload Data Handling Station – Kiruna
PDS	Payload Data Segment
PEB	Payload Equipment Bay
PLSOL	Payload Switch off Line

PMC	Payload Module Computer
PRNU	Pixel Response Non Uniformity
PSO	On-Orbit Position
QC	Quality Control
QUARC	Quality Analysis and Reporting Computer
QWG	Quality Working Group
RIVM	Rijksinstituut voor Volksgezondheid en Milieu
RTS	Random Telegraphic Signal
SA	Service d'Aeronomie
SATU	Star Acquisition and Tracking Unit
SFA	Steering Front Assembly
SFCM	Stellar Fine Control Mode
SFM	Steering Front Mechanism
SMNA	Servicio Meteorológico Nacional de Argentina
SODAP	Switch On and Data Acquisition Phase
SPA1	Spectrometer A CCD 1
SPA2	Spectrometer A CCD 2
SPB1	Spectrometer B CCD 1
SPB2	Spectrometer B CCD 2
SPH	Specific Product Header
SQADS	Summary Quality Annotation Data Set
SSP	Sun Shade Position
SZA	Solar Zenith Angle

2 SUMMARY

During the reporting month GOMOS instrument had one not planned unavailability period on 3rd December when all the PEB subsystems were switched off and the PMC was switched down to Suspend due to a spurious PLSOL. After the uplink of a new PMC software version, the entire payload was gradually recovered: GOMOS on 5th December 04:29. Other two unavailabilities occurred on 15th and 26th December for almost three hours due to planned maneuvers (section 3.1).

The availability of level 1b data within the archives was over 97% except for the third week of the month when it decreased till 95%. The level 0 availability is very stable being the percentage situated almost at 100% (section 3.3).

The detector temperatures during December are similar to the ones registered in November and about one degree higher than December 2002. The expected seasonal variation of the temperatures with amplitude of around one degree can be clearly observed (section 4.2).

The elevation MIP has a significant variation till 12th December 2003 when a new PSO algorithm was activated in order to reduce the deviations of the ENVISAT platform attitude with respect to the nominal one. The amplitude of the MIP displacement seems now to be much smaller and will be carefully monitored in order to assess if the algorithm is working well (section. 4.5.3).

The variation of the radiometric sensitivity ratio is outside the threshold for some photometer ratios and for some stars. ACRI ESL has performed some investigations (still on going) and two possible causes

have been identified up to now: the vignetting correction and an inaccurate reflectivity correction LUT. Future monthly reports will include the latest news on this issue (section 5.4.1).

On 10th and 17th December new calibration ADF's were disseminated with updated DC maps of orbits 09273 and 09380 respectively (section 5.1.2).

ESA has continued the supply of selected data products to validation teams using the prototype processor at ACRI. An upgrade of the data processing algorithm specification is in progress, in order to improve both level 1 and level 2 products.

3 INSTRUMENT UNAVAILABILITY

3.1 GOMOS Unavailability Periods

In table 3.1-1 there is a list of GOMOS unavailability reports issued during the period 1st December (00:00:00) 2003 until 31st December (24:00:00) 2003. On 3rd December all the PEB subsystems (GOMOS among them) were switched off and the PMC was switched down to Suspend due to a spurious PLSOL. This PLSOL was caused by the known PMC software "select-start recursion" problem associated to a MIPAS switch-down shortly before (for unknown reasons since the MIPAS ICU was switched off by the PLSOL and hence its memory contents were lost). It was agreed to uplink the new PMC software version that includes the fix to the "select-start recursion" bug. The PMC was then restarted successfully, followed by the gradual recovery of the full payload (GOMOS recovery occurred on 5th December 04:29).

The second GOMOS unavailability report (15th and 26th December) was related to some Orbit Control Manoeuvres and hence, the unavailability periods were planned.

Table 3.1-1: List of unavailability periods issued during the reporting month

Reference of unavailability report	Unavailability Start	Unavailability Stop	Description
EN-UNA-2003/0354	3 Dec 2003 07:18:43.000 Day of Year = 337 Orbit = 09193 Anx Offset = 0436.287	5 Dec 2003 04:29:03.000 Day of Year = 339 Orbit = 09220 Anx Offset = 0086.231	PMC was switched down to Suspend due to a spurious PLSOL
EN-UNA-2003/0370	15 Dec 2003 19:25:00.000 Day of Year = 349 Orbit = 09372 Anx Offset = 0382.175	15 Dec 2003 22:20:00.000 Day of Year = 349 Orbit = 09373 Anx Offset = 4846.247	Planned: for the duration of the manoeuvre (SFCM) GOMOS was commanded to Heater mode with MDE Off then returned to an operational state (PAUSE with SFA calibrated) at 22.20.00.000. Again it was commanded to Heater mode on 26-DEC-2003 18:39 and resumed operations at 22.20.00 of the same day.

3.2 Stars Lost in Centering

The acquisition of a star initiates with a rallying phase where the telescope mechanism is directed towards the expected position of the star. Subsequently the acquisition procedure enters into detection mode, where the SATU star tracker output signal is pre-processed for spot presence survey and for the location of the most illuminated couple of adjacent pixels for two added lines, over the detection field. The Most Illuminated Pixel (MIP) defines the position of the first SATU centering window. The next step in the acquisition sequence is then initiated and consists of a centering phase where the SATU output signal is pre-processed for spot presence survey over the maximum of 10x10 pixel field. This allows the third phase to begin: the tracking phase.

The centering phase has occasionally resulted in loss of the star from the field of view. The fig. 3.2-1 reports the percentage of the stars lost in centering for the period 03-FEB-2003 to 04-JAN-2004. It can be seen that five stars, mainly weak stars (higher star id means higher magnitude) are lost during centering phase in more than 5% of their planned observations. As the monitoring shows neither trend nor excessively high percentages of loss, there is no need for the moment to reject any star from the catalogue, and there is no indication of instrument-related problems. However, as the star number 109 was planned to be occulted 116 and was lost 8 times in the period 15 December – 04 January, this results in a relatively high percentage of loss that will be monitored during the following months.

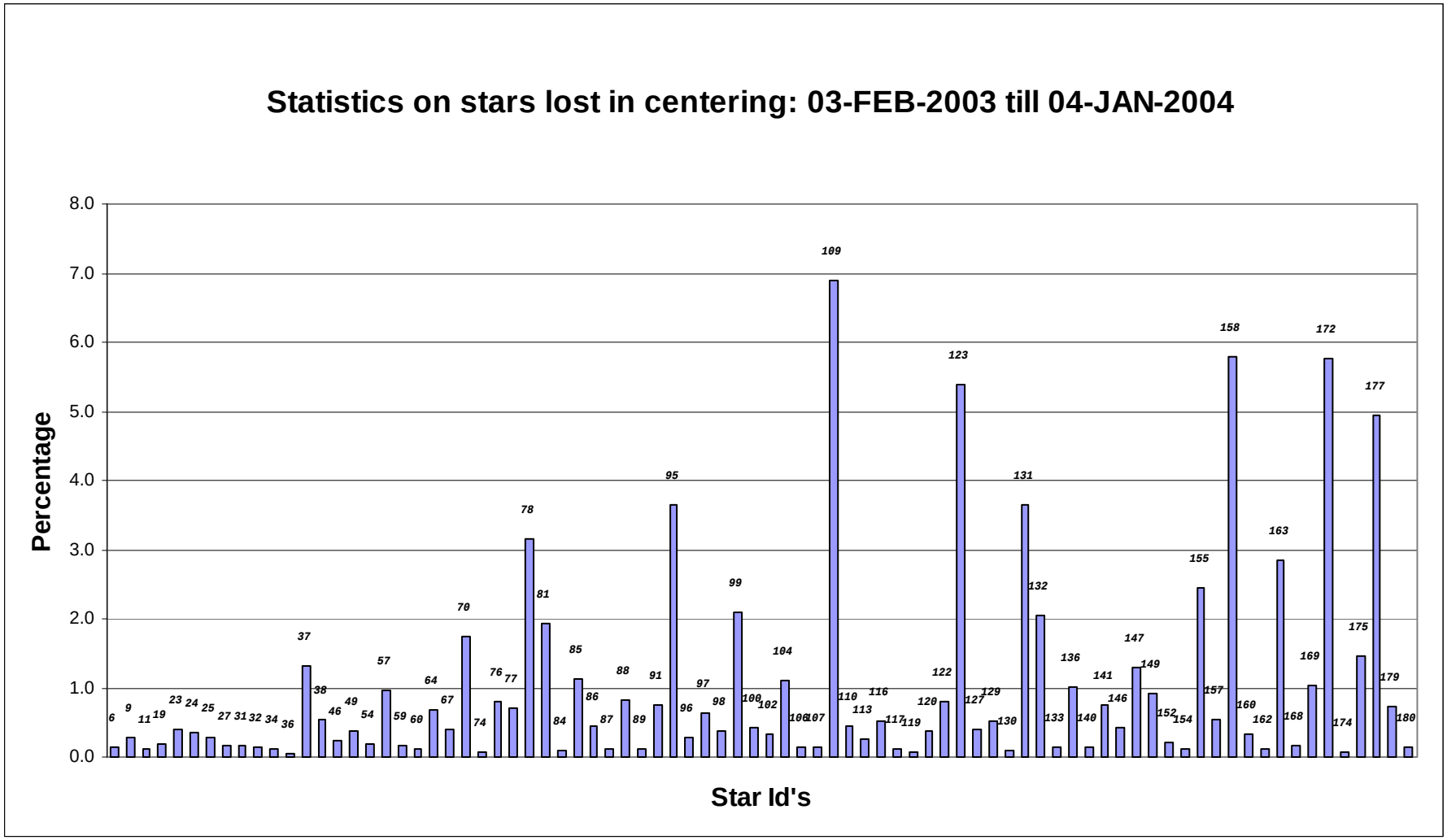

Figure 3.2-1: Statistics on stars that have been lost during the centering phase. The numbers above the columns correspond to the Star Id's

3.3 Data Generation Gaps

The trend in percentage of available data within the archives PDHS-K and PDH-E is depicted in fig. 3.3-1 (when instrument was in operation). It is a good indicator on how the PDS chain is working in terms of generation and dissemination of data to the archives. The percentage is calculated once per week.

The availability of level 1b data within the archives was over 97% except for the third week of the month when it decreased till 95%. The level 0 availability is very stable being the percentage situated almost at 100%.

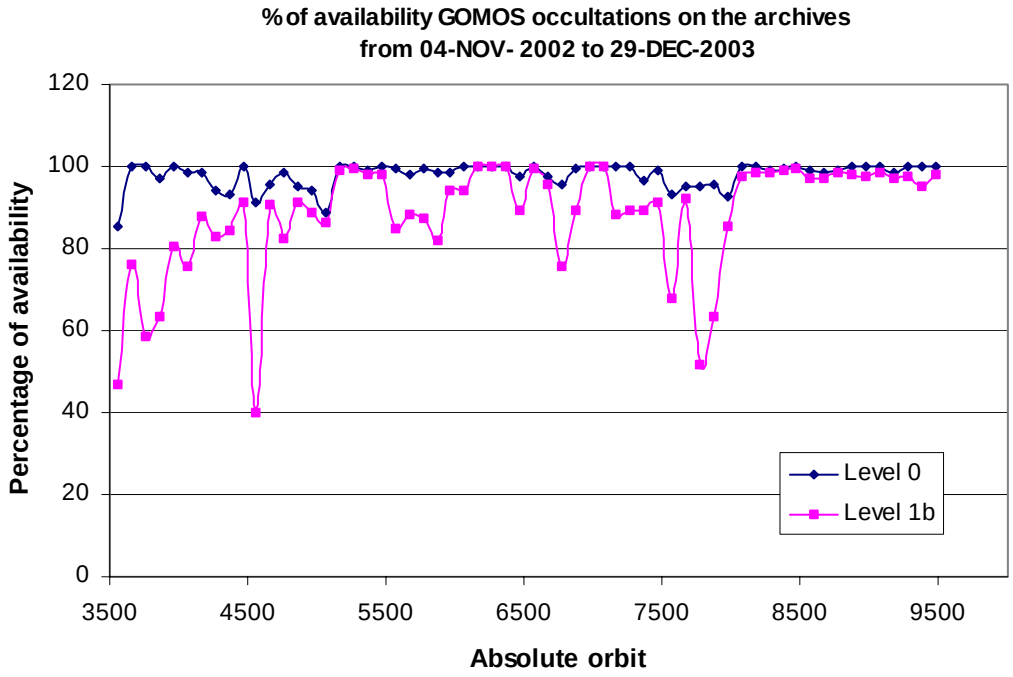

Figure 3.3-1: Percentage of level 0 and level 1b data availability on the archives PDHS-E and PDHS-K

3.3.1 LEVEL 0 PRODUCTS: GOM_NL__0P

Occultations planned to be acquired but for which no GOM_NL__0P data product has become available are presented in fig. 3.3-2 for the reporting month.

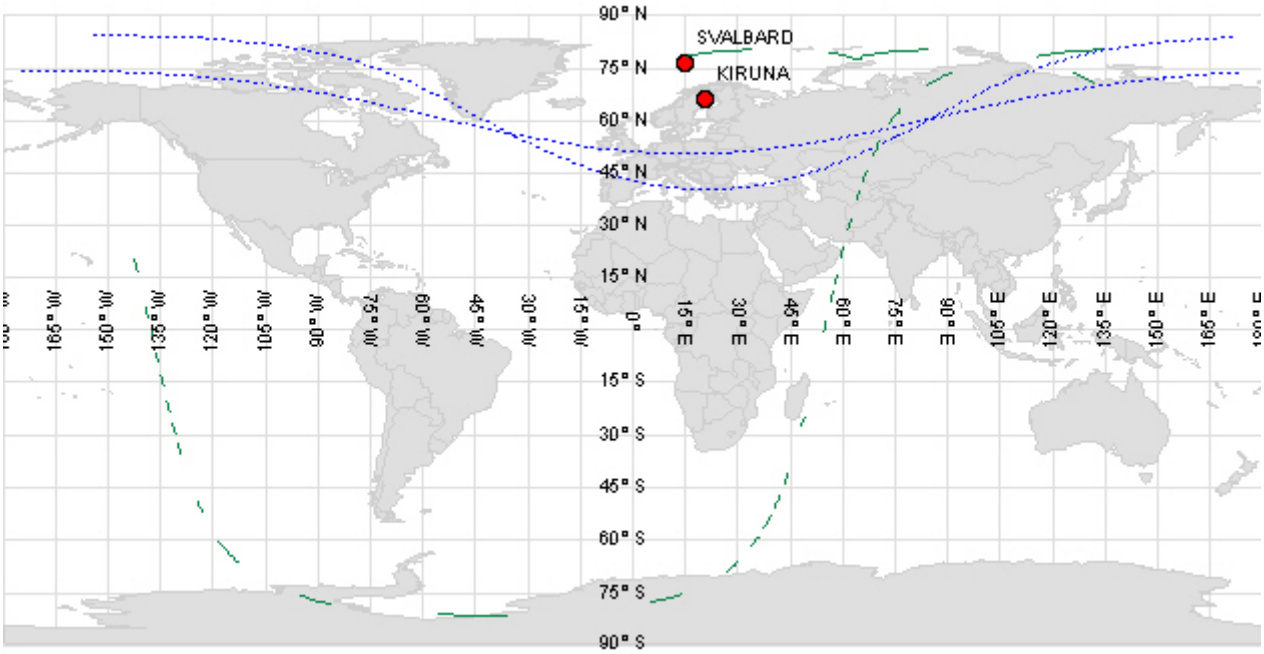

Figure 3.3-2: Orbit segments corresponding to planned data acquisitions for which no GOMOS level 0 product has become available

3.3.2 HIGHER LEVEL PRODUCTS

Routine dissemination of higher-level products produced by the PDS to Cal/Val teams and other users is enabled. Currently ESA provides the Cal/Val teams with selected products that are generated with the prototype processor developed and operated by ACRI.

4 INSTRUMENT CONFIGURATION AND PERFORMANCE

4.1 Instrument Operation and Configuration

Since end of March 2003 the instrument has suffered some changes in the minimum azimuth range configuration in order to avoid the anomaly "Voice_coil_command_saturation" that caused the instrument to go into STAND BY/REFUSE mode. Since the change to the redundant chain B on July 2003, the full range in azimuth has been again used (table 4.1-1).

Table 4.1-1: Historical changes in Azimuth configuration

Date	Orbit	Minimum Azimuth
29-MAR-2003 17:40	5635	0.0
31-MAY-2003 06:22	6530	+4.0
16-JUN-2003 16:17	6765	+12.0
15-JUL-2003 01:39	7200	-10.8

The operations of the instrument in other modes than occultation mode are identified in table 4.1-2.

There was no new Configurable Table Interface (CTI) uploaded to the instrument. The files used since the beginning of the mission are in table 4.1-3.

Table 4.1-2: GOMOS operations during December 2003

UTC time	Start orbit	Stop orbit	Mode (Asynchronous or Synchronous)	Calibration (CAL) or Dark Sky Area (DSA)
06 Dec 2003 03:55:54	9234	9241	A	CAL56
13 Dec 2003 03:35:47	9334	9334	A	DSA85
20 Dec 2003 03:15:39	9434	9434	A	DSA86
27 Dec 2003 02:55:32	9534	9534	A	DSA87

Table 4.1-3: Historic CTI Tables

CTI filename	Dissemination to FOCC
CTI_SMP_GMVIEC20030716_123904_00000000_00000004_20030715_000000_20781231_235959.N1	16-JUL-2003
CTI_SMP_GMVIEC20021104_075734_00000000_00000003_20021002_000000_20781231_235959.N1	06-NOV-2003
CTI_SMP_GMVIEC20021002_082339_00000000_00000002_20021002_000000_20781231_235959.N1	07-OCT-2003
CTI_SMP_GMVIEC20020207_154455_00000000_00000000_20020301_032709_20781231_235959.N1	21-FEB-2002

4.2 Thermal Performance

Since the beginning of the mission the hot pixel and RTS phenomena (see section 4.4.1) are producing a continuous increase of the dark charge signal within the CCD detectors. In order to minimize this effect, three successive CCD cool down were performed in orbits 800 (25th April 2002), 1050 (13th May 2002) and 2780 (11th September 2002) with a total decrease in temperature of 14 degrees.

Fig. 4.2-1 and 4.2-2 display, respectively, the overall temperature variation and the temperature variation around the Ascending Node Crossing (ANX) time with a resolution of 0.4 degrees (coding accuracy for level 0 data). The CCD temperatures during December are similar to the ones registered in November and about one degree higher than December 2002. The expected seasonal variation of the temperatures with amplitude of around one degree can be clearly observed. The peaks that occur mainly in spectrometer B1 and B2 are also to be noted. They happen a little before the ANX for some consecutive orbits and every 8-10 days. Their origin is still not known, as we did not find any correlation between these peaks and other activities carried out by other ENVISAT instruments. The CCD temperature at almost the same latitude location (fig. 4.2-2) is monitored in order to detect any inter-orbital temperature variation.

The decrease observed on 24th March 2003, twice in September 2003 and at the beginning of December 2003 in all detectors is after GOMOS switch off periods, when the instrument did not have enough time to reach the nominal temperature before starting the measurements.

The orbital temperature variation of the detector SPB2 (fig. 4.2-3 & 4.2-4) is bigger than nominal because GOMOS started to measure before reaching the nominal thermal configuration after the switch off

periods. The maximum difference was around 3.3 degrees. The stability of the temperature during the orbit is important because it affects the position of the interference patterns. The phenomenon of the interference is present mainly in SPB and this Pixel Response Non-Uniformity (PRNU) is corrected during the processing.

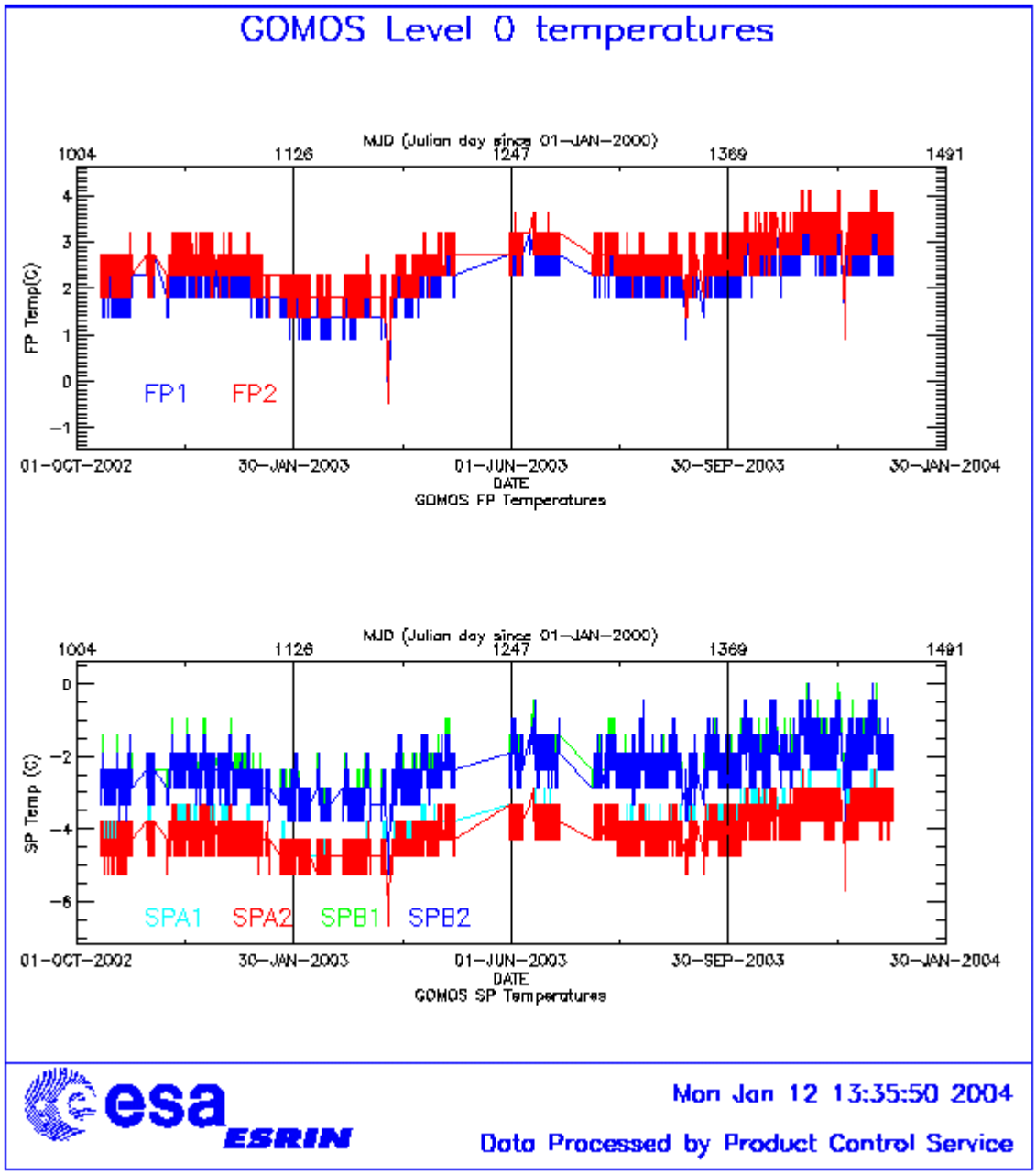

Figure 4.2-1: Level 0 temperature evolution of all GOMOS CCD detectors from October 2002 until end of December 2003

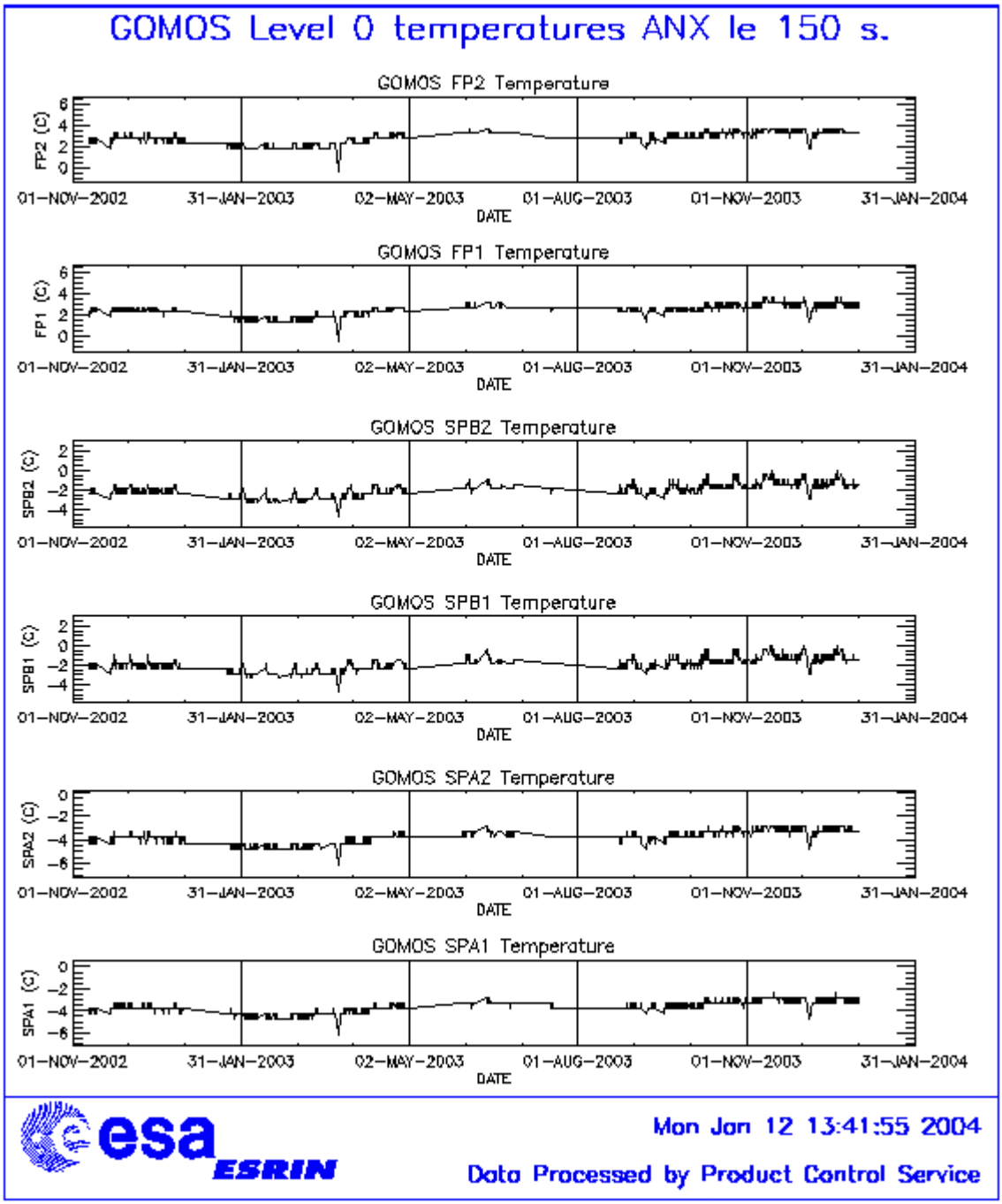

Figure 4.2-2: **Level 0 temperature evolution of all GOMOS CCD detectors around ANX from November 2002 until end of December 2003**

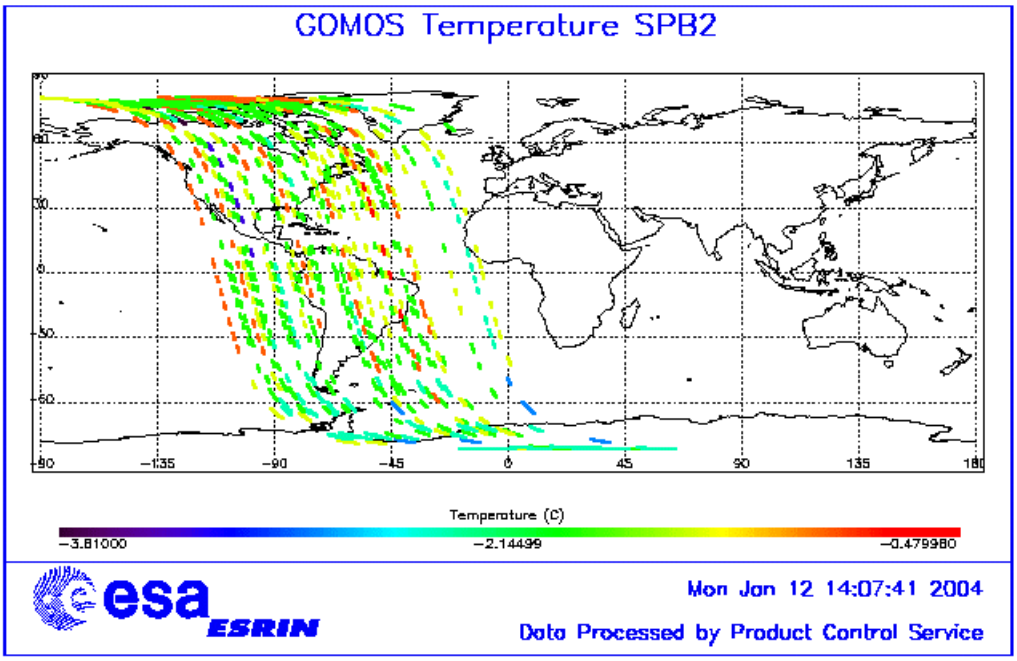

Figure 4.2-3: Ascending orbital variation of SPB2 temperature during some orbits on December 2003

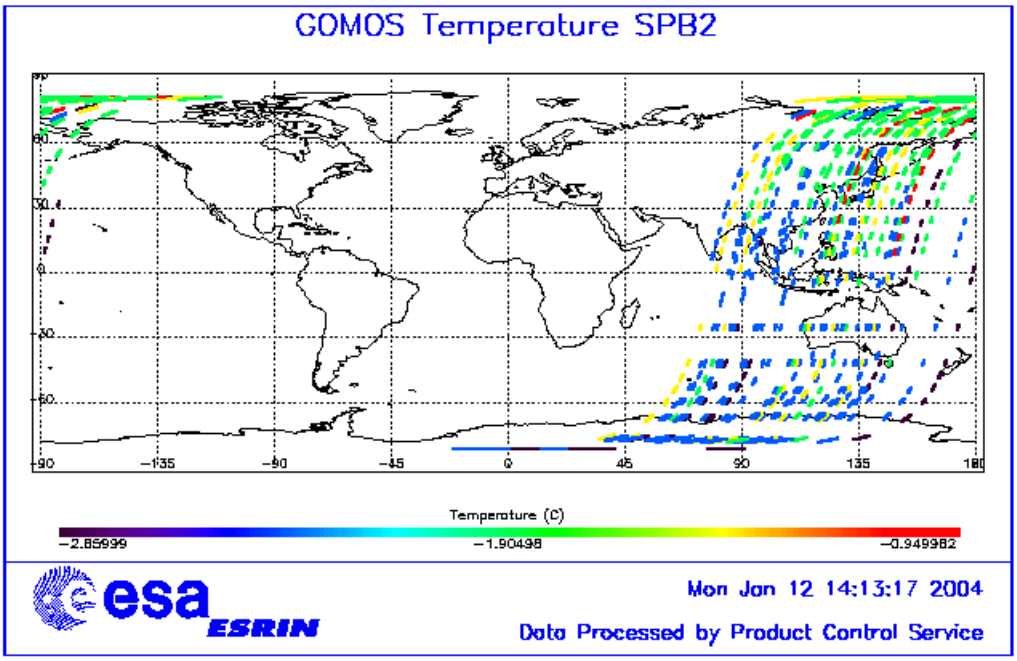

Figure 4.2-4: Descending orbital variation of SPB2 temperature during some orbits on December 2003

4.3 Optomechanical Performance

No new band setting calibration has been performed during December. These results were already presented in previous versions of the MR (last calibration analysis done in November 2003).

The position of stellar spectra of star id 2, 9 and 29 observed in dark-limb spatial spread monitoring mode have been averaged above 120 km altitude, and compared to the average positions obtained during the last calibration (blue dots in fig. 4-3.1) performed at the beginning of August after the transition to redundant chain. In table 4.3-1 the mean values of the location of the star signal for all the calibration analysis done till now are reported. The 'left' and 'right' values are calculated (the whole interval is not used) because the spectra present a slight slope, more pronounced in the spectrometer B (see fig. 4-3.1). The current processors GOMOS IPF 4.00 and GOPR prototype 5.4 still expect the spectra to be aligned along CCD lines, and therefore use only a single average line index per CCD. The values currently implemented of 81, 80, 82, 82 for SPA1, SPA2, SPB1 and SPB2 are still compatible with the observed 'left' and 'right' average position. The lookup table implemented in the version 6.0 of the prototype level 1 processor has been updated in order to have the line index as a function of the wavelength.

In table 4.3-2, mean values of the location of the star signal are calculated for some specific wavelength intervals. These intervals have been changed between the calibration performed in September 2002 and the ones performed afterwards. The results obtained are very similar to the ones obtained in previous exercises. Table 4.3-3 reports the average location of the star spot on the photometer 1 and 2 CCD. No difference has been found for both photometers in column and in row positions.

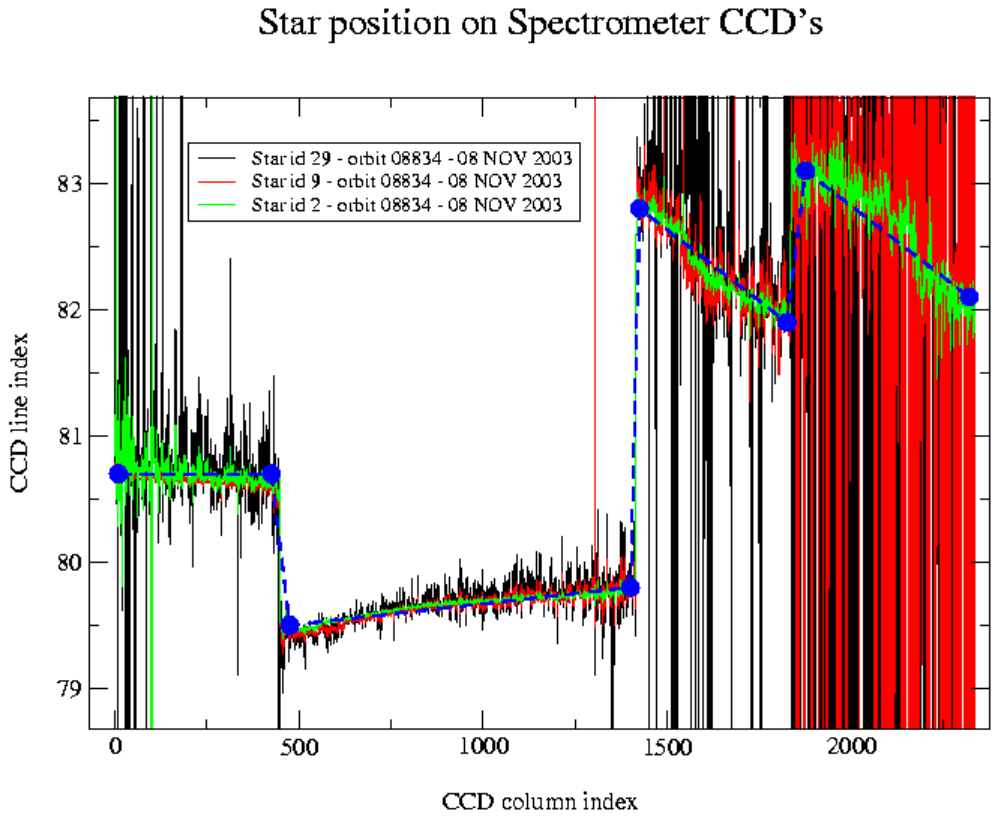

Figure 4.3-1: Average position of star spectra on the CCD

Table 4.3-1: Mean value of the location of the star signal during the occultation at the edges of every band (mean over 50 values, filtering the outliers)

	UV (SPA1) left/right	VIS (SPA2) left/right (Inverted spectra)	IR1 (SPB1) left/right	IR2 (SPB2) left/right
11/09/2002	80.7/80.7	79.8/79.5	82.8/81.9	83.1/82.1
01/01/2003	80.7/80.6	79.8/79.5	82.8/82.0	83.2/82.2
17/07/2003 & 02/08/2003	80.7/80.7	79.8/79.5	82.8/81.9	83.1/82.1
08/11/2003	80.7/80.6	79.8/79.5	82.8/81.9	83.1/82.1

Table 4.3-2: Mean value of the location of the star signal during the occultation (as table 4.3-1) but now within some wavelength intervals

	UV (SPA1)	VIS (SPA2)	IR1 (SPB1)	IR2 (SPB2)
11/09/2002 wl range (nm)	80.8 [300-330]	79.8 [500-530]	82.6 [760-765]	82.9 [937-942]
01/01/2003 wl range (nm)	80.6 [350-360]	78.6 [650-670]	81.6 [760-765]	80.3 [935-945]
02/08/2003	80.6	79.7	82.5	82.8
08/11/2003	80.6	79.9	82.4	82.8

Table 4.3-3: Average column and row pixel location of the star spot on the photometer CCD during the occultation

	FP1 (column/row)	FP2 (column/row)
11/09/2002	11/4	5/5
01/01/2003	10/4	6/4.9
02/08/2003	10/4	6/5
08/11/2003	10/4	6/5

4.4 Electronic Performance

4.4.1 DARK CHARGE EVOLUTION AND TREND

The trend of Dark Charge (DC) is of crucial importance for the final quality of the products, and is therefore subject to intense monitoring. As part of the DC there is:

1 "Hot pixels", a pixel is "hot" when its dark charge exceeds its value measured on ground, at the same temperature, by a significant amount.
2 RTS phenomenon (Random Telegraphic Signal), it is an abrupt change (positive or negative) of the CCD pixel signal, random in time, affecting only the DC part of the signal and not the photon generated signal.

The temperature dependence of the DC would make this parameter a good indicator of the DC behaviour, but the hot pixels and the RTS are producing a continuous increase of the DC (see trend in fig. 4.4-1 and 4.4-2). To take into account these phenomena, in the last version of the level 1 processor (GOMOS/4.00) operational since May 2003, a DC map per orbit is extracted from a Dark Sky Area (DSA) observation performed around ANX (full dark conditions). For every level 1b product (occultation), the actual

thermistor temperature of the CCD is used to convert the DC map measured around ANX into an estimate of the DC at the time (and different temperature) of the actual occultation. When the DSA observation is not available, the DC map inside the calibration product that was measured at a given thermistor reference temperature is used; again, the actual thermistor temperature of the CCD is used to compute the actual map. Table 4.4-1 reports the list of products that used the DC maps inside the calibration file due to the non-availability of DSA observation. A "CAL DC map with no T dep." means than, as the temperature information was not available for the occultation, the DC map used is exactly the one inside the Calibration product.

Table 4.4-1: Table of level 1b products that used the Calibration DC maps instead of the DSA observation

Product Name	DC Information
GOM_TRA_1PNPDE20031206_023719_000000662022_00161_09233_0000.N1	CAL DC map with no T dep.
GOM_TRA_1PNPDE20031206_024043_000000642022_00161_09233_0001.N1	CAL DC map used
GOM_TRA_1PNPDE20031206_024311_000000492022_00161_09233_0002.N1	CAL DC map used
GOM_TRA_1PNPDE20031206_024436_000000552022_00161_09233_0003.N1	CAL DC map used
GOM_TRA_1PNPDE20031206_024835_000000472022_00161_09233_0004.N1	CAL DC map used
GOM_TRA_1PNPDE20031206_025219_000000522022_00161_09233_0005.N1	CAL DC map used
GOM_TRA_1PNPDE20031206_025411_000000382022_00161_09233_0006.N1	CAL DC map used
GOM_TRA_1PNPDE20031206_025625_000000402022_00161_09233_0007.N1	CAL DC map used
GOM_TRA_1PNPDE20031206_025851_000000382022_00161_09233_0008.N1	CAL DC map used
GOM_TRA_1PNPDE20031206_030054_000000372022_00161_09233_0009.N1	CAL DC map used
GOM_TRA_1PNPDE20031206_030222_000000392022_00161_09233_0010.N1	CAL DC map used
GOM_TRA_1PNPDE20031206_030459_000000382022_00161_09233_0011.N1	CAL DC map used
GOM_TRA_1PNPDE20031206_030622_000000392022_00161_09233_0012.N1	CAL DC map used
GOM_TRA_1PNPDE20031206_031229_000000342022_00161_09233_0013.N1	CAL DC map used
GOM_TRA_1PNPDE20031206_031711_000000402022_00161_09233_0014.N1	CAL DC map used
GOM_TRA_1PNPDE20031206_031844_000000462022_00161_09233_0015.N1	CAL DC map used
GOM_TRA_1PNPDE20031206_032017_000000492022_00161_09233_0016.N1	CAL DC map used
GOM_TRA_1PNPDE20031206_032214_000000392022_00161_09233_0017.N1	CAL DC map used
GOM_TRA_1PNPDE20031206_032428_000000542022_00161_09233_0018.N1	CAL DC map used
GOM_TRA_1PNPDE20031206_032728_000000522022_00161_09233_0019.N1	CAL DC map used
GOM_TRA_1PNPDE20031206_033032_000000372022_00161_09233_0020.N1	CAL DC map used
GOM_TRA_1PNPDE20031206_033306_000000372022_00161_09233_0021.N1	CAL DC map used
GOM_TRA_1PNPDE20031206_033734_000000952022_00161_09233_0022.N1	CAL DC map used
GOM_TRA_1PNPDE20031206_034130_000000532022_00161_09233_0023.N1	CAL DC map used
GOM_TRA_1PNPDE20031206_034623_000000492022_00161_09233_0024.N1	CAL DC map used
GOM_TRA_1PNPDE20031206_034758_000000492022_00161_09233_0025.N1	CAL DC map used
GOM_TRA_1PNPDE20031206_034937_000000412022_00161_09233_0026.N1	CAL DC map used
GOM_TRA_1PNPDE20031206_035136_000000402022_00161_09233_0027.N1	CAL DC map used
GOM_TRA_1PNPDE20031206_035327_000000392022_00161_09233_0028.N1	CAL DC map used
GOM_TRA_1PNPDE20031206_035452_000000512022_00161_09233_0029.N1	CAL DC map used
GOM_TRA_1PNPDE20031206_035630_000000392022_00162_09234_0030.N1	CAL DC map used

In fig. 4.4-1 and 4.4-2 it is plotted the average DC inserted by the processor into the level 1b data products for the spectrometers SPA1 and SPB2 (per band: upper, central and lower). From the figures, it can be noted that the rate of increase of DC for the last two months, November/December, is rather stable.

The same DC values are plotted in fig. 4.4-3 but only for some occultations during the reporting period.

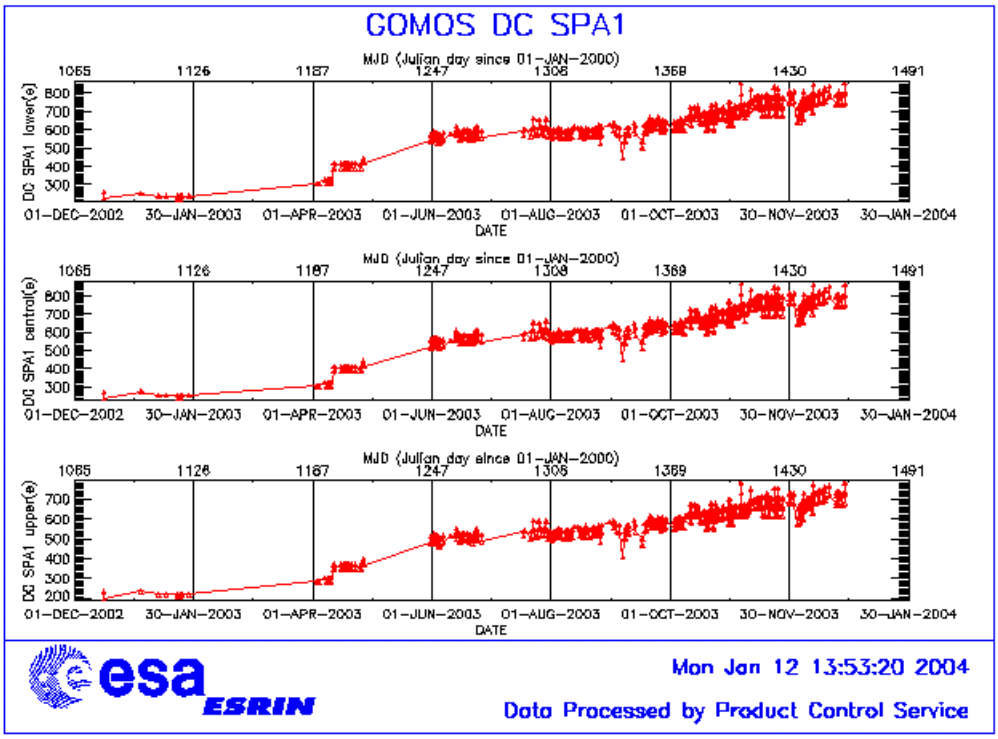

Figure 4.4-1: Mean DC evolution on SPA1 from 15th December 2002 until end of December 2003

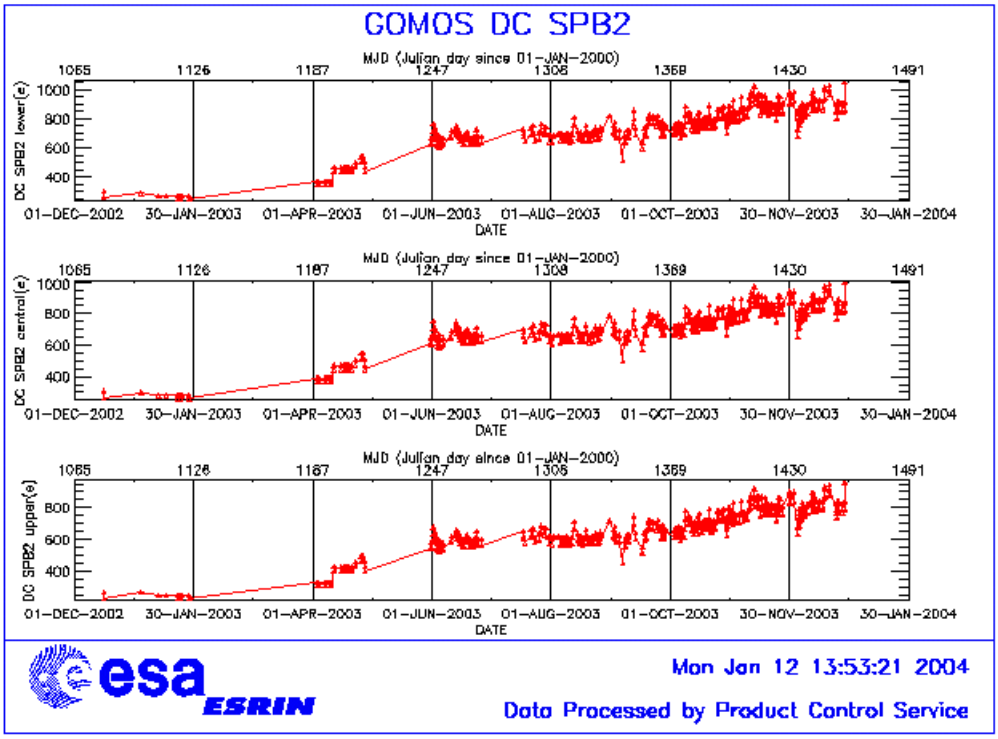

Figure 4.4-2: Mean DC evolution on SPB2 from 15th December 2002 until end of December 2003

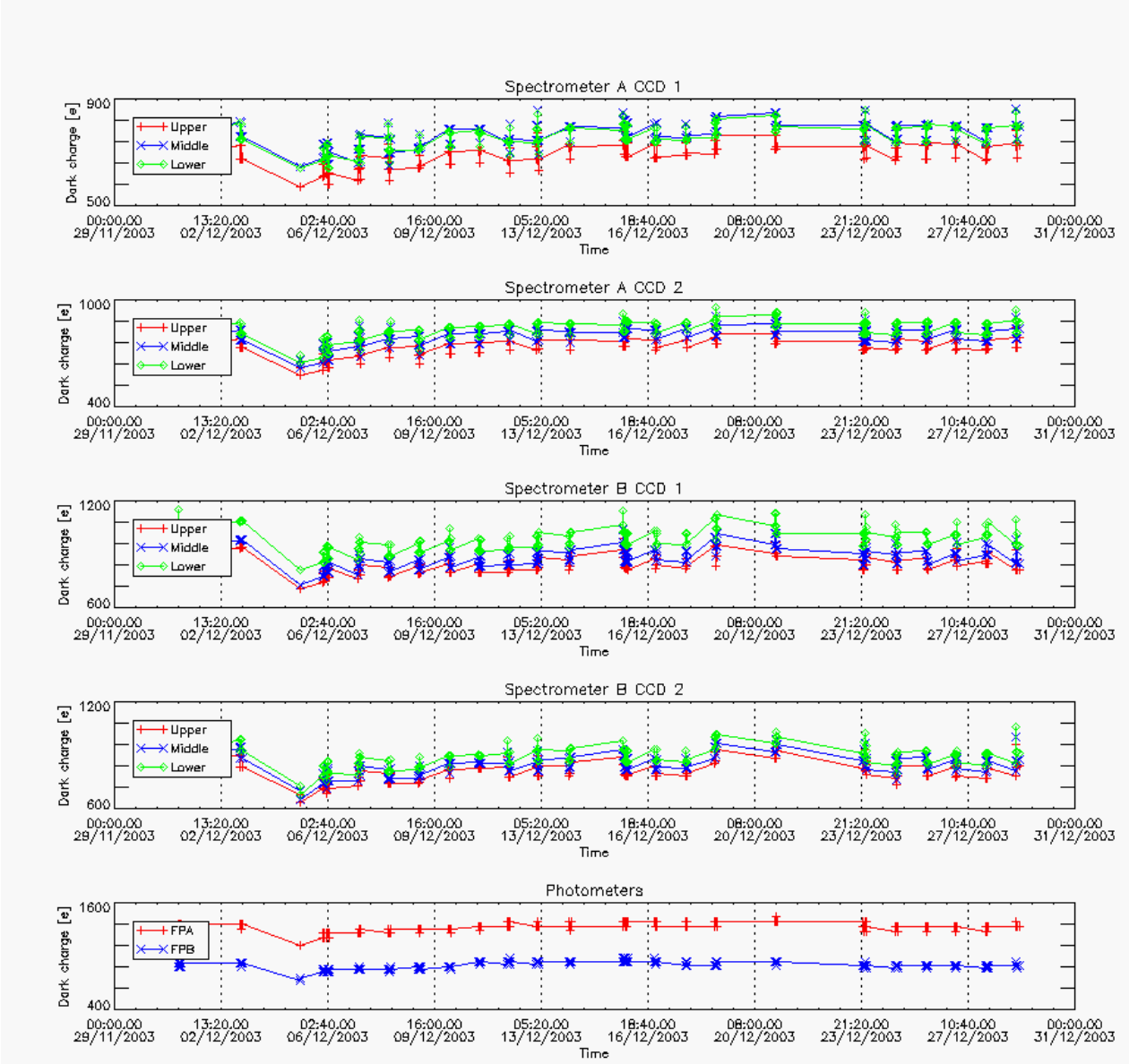

Figure 4.4-3: Mean Dark Charge of spectrometers and photometers during reporting month

4.4.2 SIGNAL MODULATION

A parasitic signal was found to be systematically present, added to the useful signal, at least for spectrometers A1 and A2. The modulation is corrected in the data processing, but the modulation signal standard deviation is routinely monitored in order to detect any trend (fig. 4.4-4).

The modulation standard deviation, for every spectrometer, is characterised as follows:

$$\sigma_{mod} = (\text{'static noises'} - \text{'total static variance'})^{1/2} / \text{gain} \qquad \text{(in ADU)}$$

1 The ‘static noises’ are calculated from the DSA observation performed once per orbit
The ‘total static variance’ is obtained from ADF data (electronic chain noise, quantization noise).

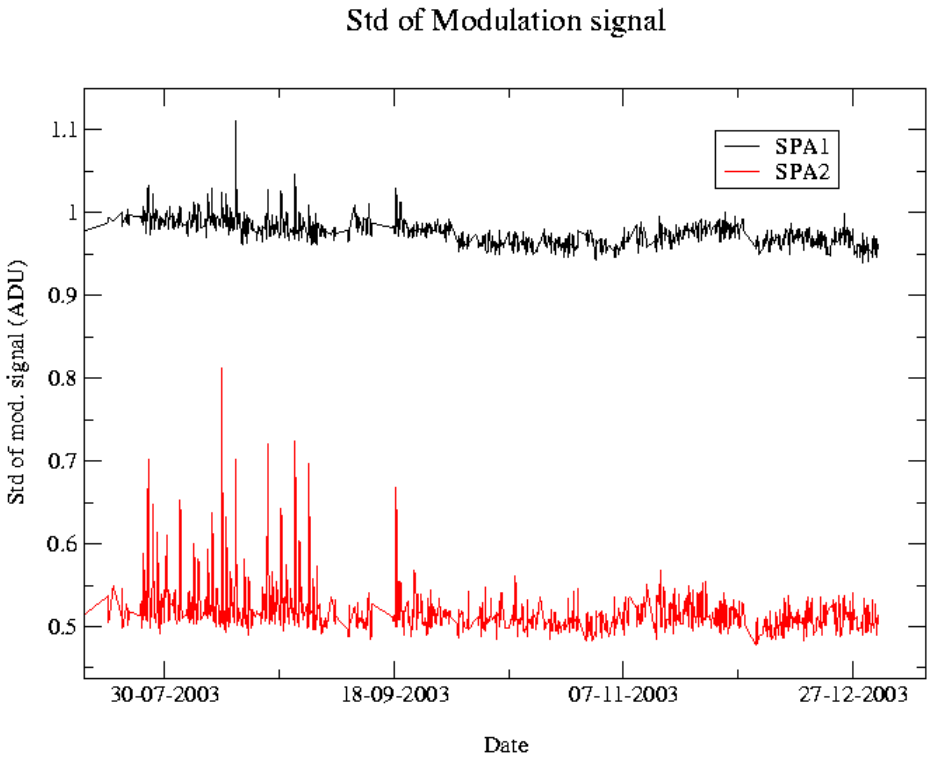

Figure 4.4-4: Standard deviation of the modulation signal

4.4.3 ELECTRONIC CHAIN GAIN AND OFFSET

No new electronic chain gain and offset calibration has been done during the reporting month so these results have been already presented in previous MR.

The routine monitoring of the ADC offset is a good indicator of the ageing of the instrument electronics. During the definition of this routine activity, an exercise has been done to analyze the variation of the ADC offset using the calibration observation in linearity mode (orbits 2810, 4384, 4834, 5219 and 5734). The fig. 4.4-5 presents the evolution of the calibrated ADC offset for each spectrometer electronic chain. The unexpected increase of this offset seems to be due to an external contribution. In the ADC offset calibration procedure, linearity observations are used with two integration times of 0.25 and 0.50 seconds to extrapolate to an integration time of 0 seconds that give the complete chain offset and not only the ADC offset. The complete offset contains any possible offsets, and especially the static dark charge (i.e. the dark charge that does not depend of the spectrometer integration time). If the memory area of the CCD is affected by the generation of hot pixels (this is confirmed by the presence of vertical lines visible in the measurement maps in spatial spread monitoring mode), it becomes that the increase observed in fig. 4.4-5 is due to these new hot pixels.

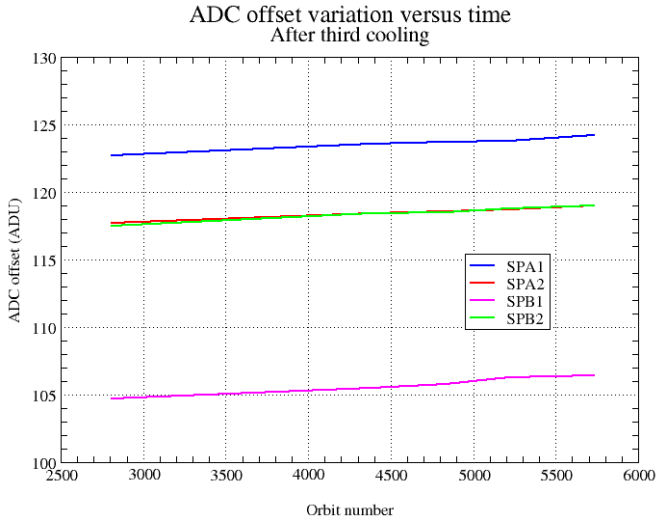

Figure 4.4-5: Evolution of the ADC offset for each spectrometer electronic chain

Next task consists in completing the analysis to confirm that the offset increase is due to the hot pixels in memory area. This can be proven by the study of the noise due to the increased dark charge. The increase of ADC offset will be assumed to be equal to the increase of 'static dark charge' and the corresponding noise will be computed and compared to the increase of the signal variance residual.

If we keep the ADC offset constant, as it is also used to compute the dark charge at band level used to correct the samples in the level 1b processing, the increase of the static dark charge - not taken into account in the ADC offset - is compensated by an artificial increase of the calibrated dark charge. So, the star and limb spectra are correctly corrected for dark charge. A small bias can be added to the instrument noise due to the incorrect dark charge level. Anyway, this quantity is not large enough to require a modification of the ADC offset value.

4.5 Acquisition, Detection and Pointing Performance

4.5.1 SATU NOISE EQUIVALENT ANGLE

The Star Acquisition and Tracking Unit (SATU) noise equivalent angle (SATU NEA) consists of the statistical angular variation of the SATU data above the atmosphere. The mean of the standard deviation (std over the 50 values per measurement) above 105 km are computed for every occultation, giving two values per occultation: one in the 'X' direction, one in the 'Y' direction. A mean value per day in every direction and limb is calculated and monitored in order to assess instrument performance in terms of star pointing. The thresholds are 2 and 3 micro radians in 'X' and 'Y' directions respectively. Before May 2003, data above 90 km have been considered (instead of 105 km) but from May 2003 on, data taken in the mesospheric oxygen layer (located around 100 km altitude) have been avoided because they could cause fluctuations on the SATU data. Also the products with errors (error flag set) are discarded from May 2003 onwards.

It can be seen in fig. 4.5-1 that the SATU NEA had some increase for bright occultations during the month but still well below the thresholds. On the contrary, for dark occultation the daily values decreased 0.2 micro radians.

The results for some occultations belonging to previous months (monthly averages) are presented in fig. 4.5-2, where no trend is visible so far.

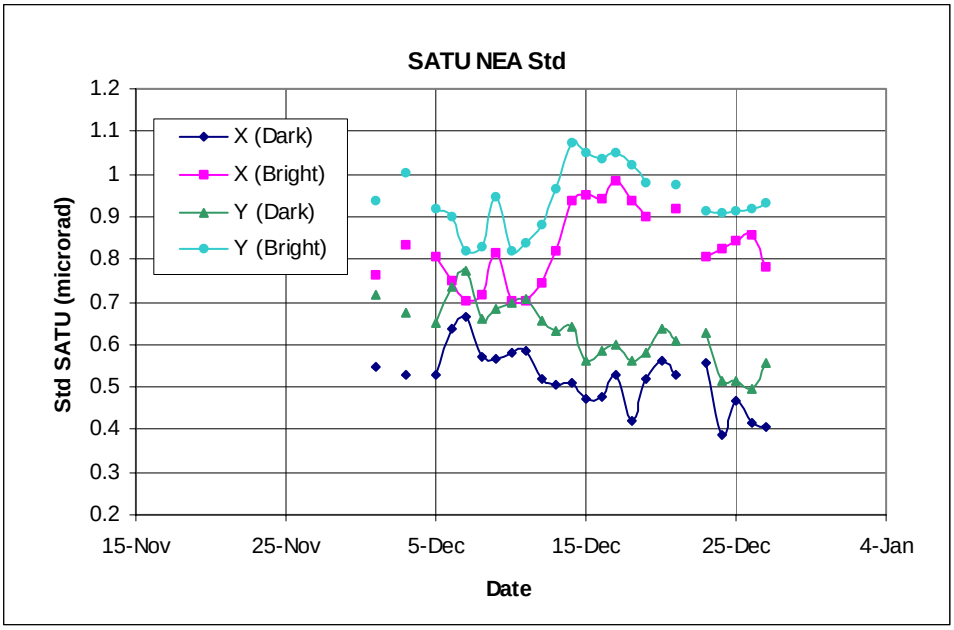

Figure 4.5-1: Average SATU per day of SATU NEA std above 105 km

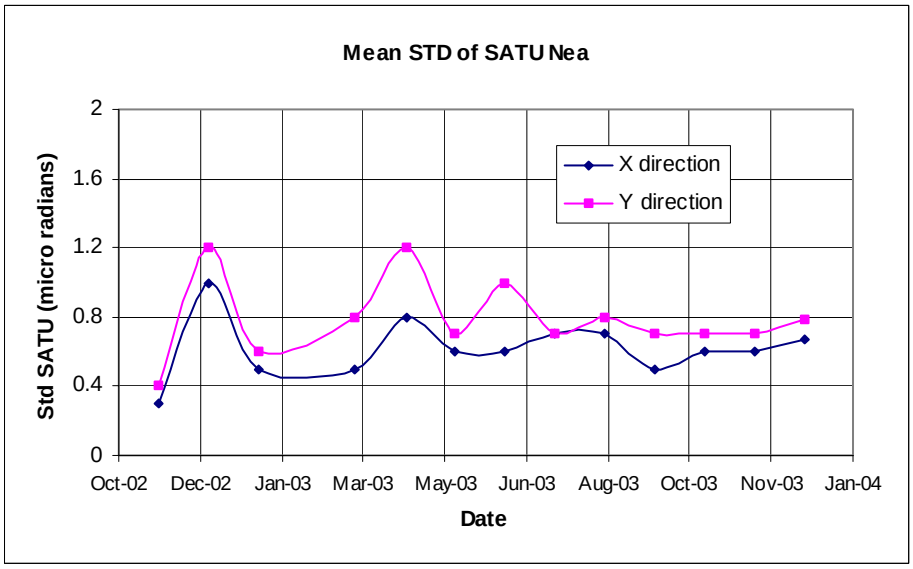

Figure 4.5-2: Average value per month of SATU NEA std above 105 km

4.5.2 TRACKING LOSS INFORMATION

This verification consists of the monitoring of the tangent altitude at which the star is lost. It is an indicator of the pointing performance although it is to be considered that star tracking is also lost due to the presence of clouds and hence not only due to deficiencies in the pointing performance. Therefore, only the detection of any systematic long-term trend is the main purpose of this monitoring. The recent results are presented in fig. 4.5-3 and fig. 4.5-4:

- The dependence of the altitude at which tracking is lost on the magnitude of the star is very small because the tracking is mainly lost due to the refraction and the scintillation that depend on the atmospheric conditions.
- There is only one star lost (twice) above 24 km altitude in dark limb (fig. 4.5-3).
- In fig. 4.5-4 there are no stars lost at high tangent altitude.
- Some statistics are given in fig. 4.5-5 calculated for a set of data and not for the whole months. For the moment, no trend is visible in the plot.

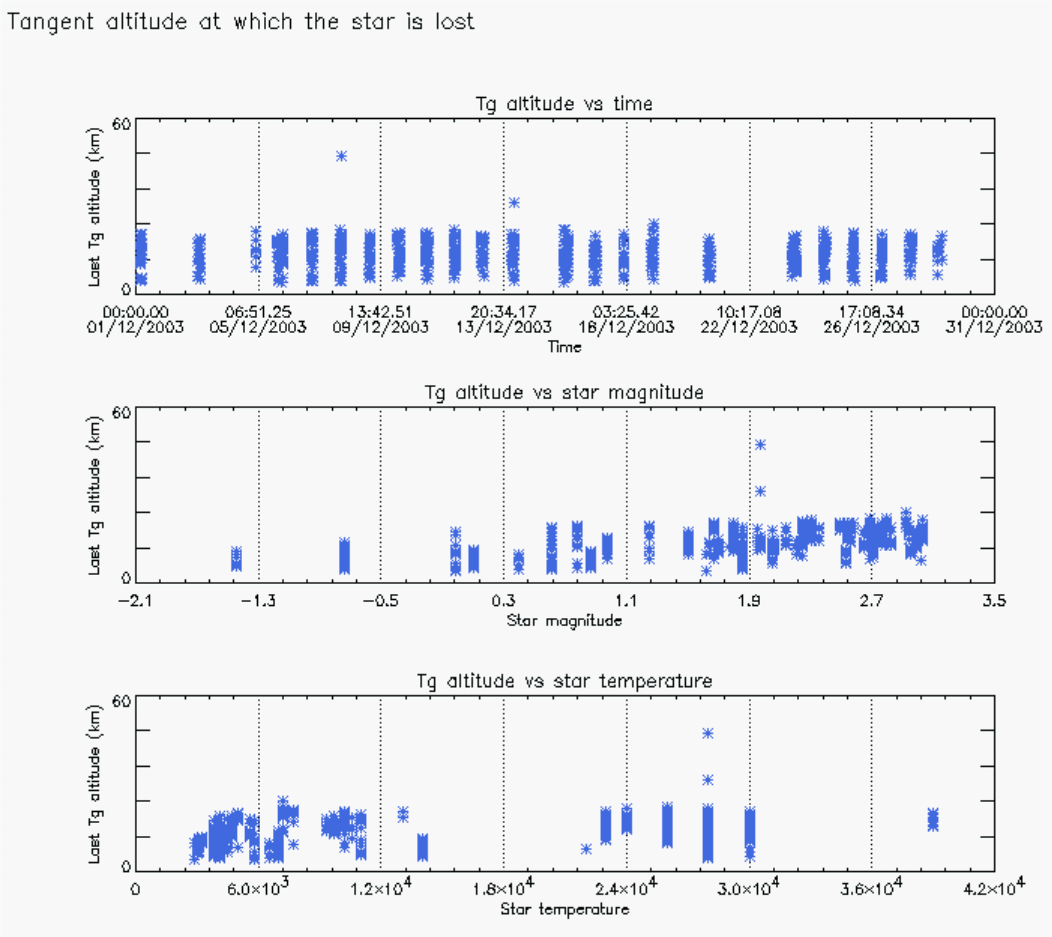

Figure 4.5-3: Last tangent altitude of the occultation (dark limb), point at which the star is lost

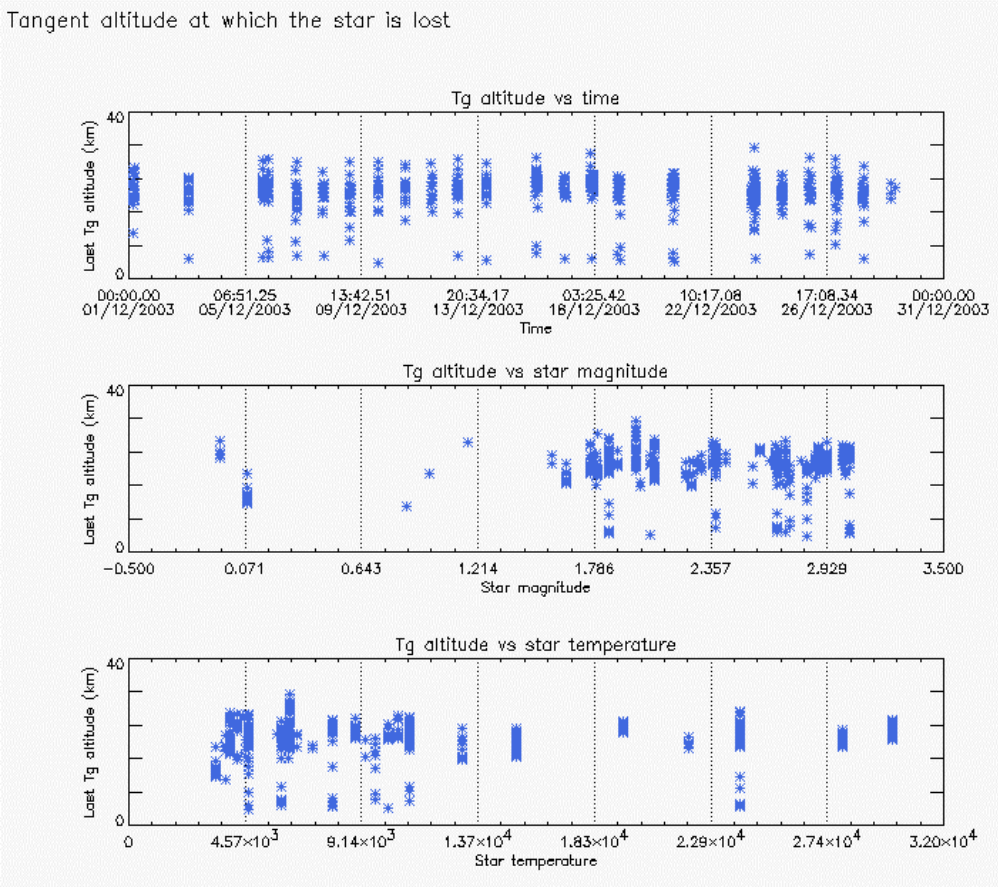

Figure 4.5-4: Last tangent altitude of the occultation (bright limb), point at which the star is lost

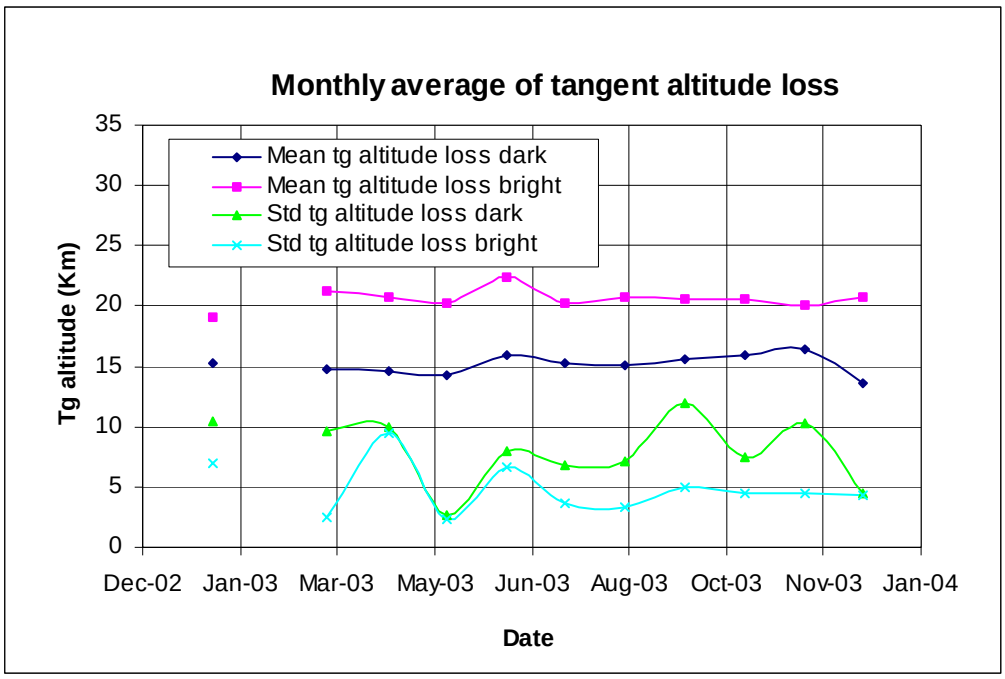

Figure 4.5-5: Monthly mean tangent altitude (and std) at which the star is lost for some occultations since January 2003

4.5.3 MOST ILLUMINATED PIXEL (MIP)

The MIP (Most Illuminated Pixel) is the star position on the SATU CCD in detection mode and it is recorded in the housekeeping data. The nominal centre of the SATU is pixel number **145** in elevation and number **205** in azimuth. The detection of the stars should not be far from this centre. As can be seen in fig. 4.5-6 the azimuth is always well within the threshold (table 4.5-1) since September 2002 even if a small variation is present. The elevation MIP has a significant variation (see the *note* below) till 12th December 2003 when a new PSO algorithm was activated in order to reduce the deviations of the ENVISAT platform attitude with respect to the nominal one. The MIP displacement will be carefully monitored in order to assess if the algorithm is working well. Fig. 4.5-7 shows the standard deviation of azimuth and elevation that should be within the thresholds of table 4.5-1. The peaks observed mean that one (or more) stars where detected very far from the SATU centre and, in this case, the star/s is lost during the centering phase (see section 3.2 for stars lost in centering).

Note: A MIP variation onto the SATU CCD of 50 pixels corresponds to a de-pointing of 0.1 degrees

Table 4.5-1: MIP Thresholds

MIP X: **Mean delta Az** **Std delta Az**	 [198 - 210] 7
MIP Y: **Mean delta El** **Std delta El**	 [145 – 154] 4

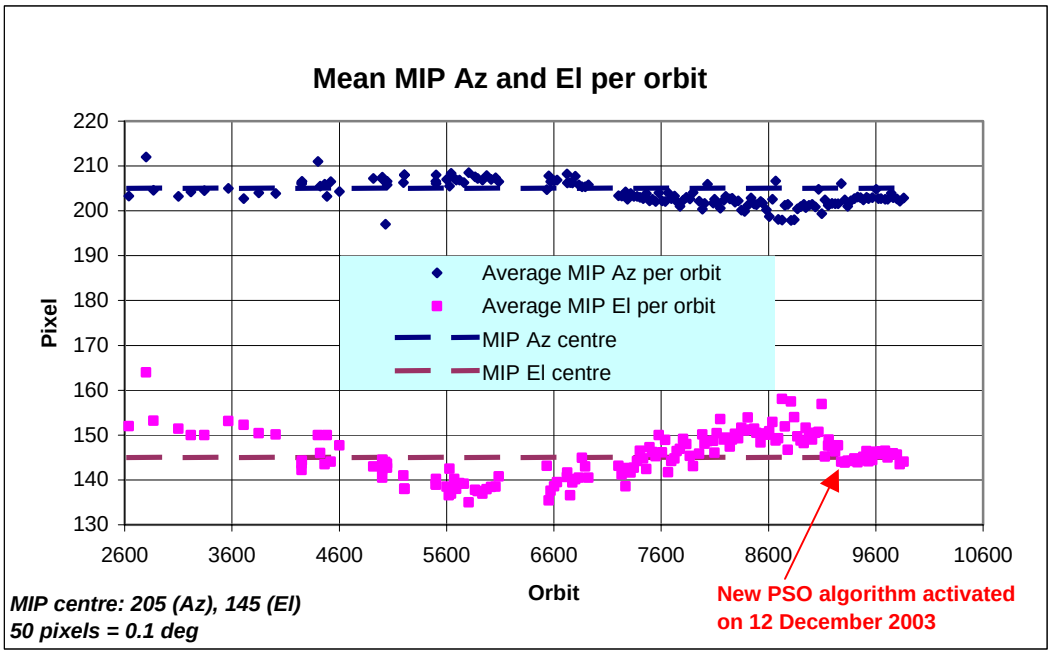

Figure 4.5-6: Mean values of MIP for some orbits since 1st September 2002 (see table 4.5-1)

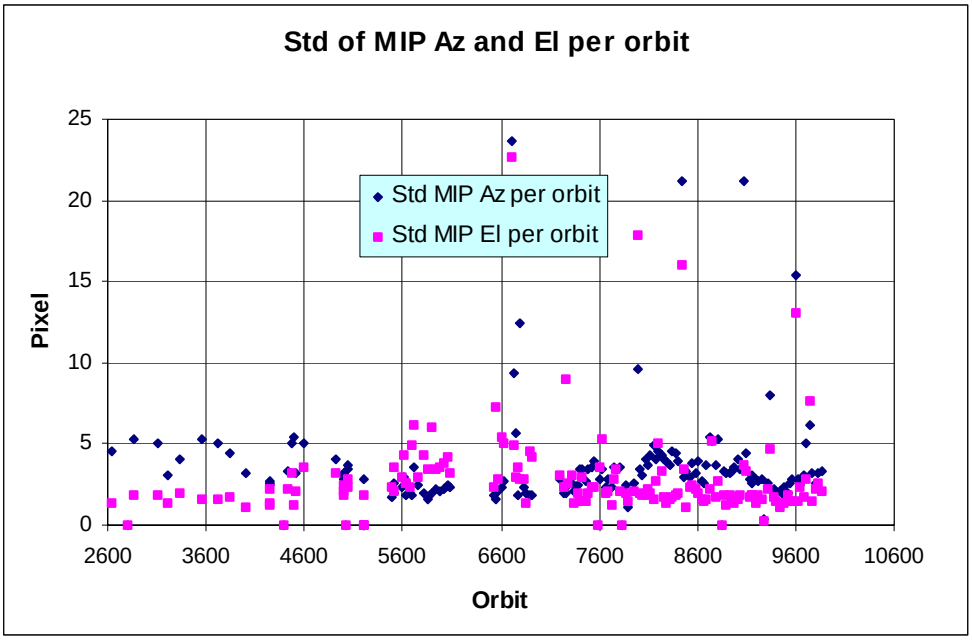

Figure 4.5-7: Standard deviation of MIP Azimuth and Elevation for some orbits since 1st September 2002 (see table 4.5-1)

5 LEVEL 1 PRODUCT QUALITY MONITORING

5.1 Processor Configuration

5.1.1 VERSION

About 19% of GOM_TRA_1P products have been received in the PCF for routine quality control and long term trend quality monitoring. The current level 1 processor software version for the operational ground segment is GOMOS/4.00 (see table 5.1-1) and the product specification is PO-RS-MDA-GS2009_10_3H. This processor has been cleared for initial level 1 data release, with a disclaimer for known artefacts that are currently being resolved and will be implemented in the next release (http://envisat.esa.int/dataproducts/availability).

Cal/Val teams are supplied with selected data sets generated by the prototype processor GOPR 5.4. See table 5.1-2 for prototype level 1b versions and modifications.

Table 5.1-1: PDS level 1b product version and main modifications implemented

Date	Version	Description of changes
31-MAY-2003	Level 1b version 4.00 at PDHS-E and PDHS-K	Algorithm baseline level 1b DPM 5.4: • Modulation correction step added after the cosmic rays detection processing • Inversion of the non-linearity and offset corrections • Modification of the computation of the estimated background signal measured by the photometers: use the spectrometer radiometric sensitivity curve and the photometer transfer function. • Use of the dark charge map at orbit level computed from the DSA (dark sky area) if any in the level 0 product • Implementation of a new unfolding algorithm for the photometer samples • See ref. [2] for more details
21-NOV-2002	Level 1b version 3.61 at PDHS-E and PDHS-K	Algorithm baseline DPM 5.3: • Review of some default values • New definition of one PCD flag (atmosphere) • Temporal interpolation of ECMWF data • See ref. [2] for more details

Table 5.1-2: GOPR level 1b product version and main modifications implemented

Date	Version	Description of changes
25-JUL-2003	GOPR 5.4f	• The demodulation process is applied only in full dark limb and twilight limb conditions.
17-JUL-2003	GOPR 5.4e	• Sun zenith angle is computed in the geolocation process. The occultation is now classified into (0) full dark limb condition, (1) bright limb condition and (2) twilight limb condition. • No background correction applied in full dark limb condition. The location of the image of the star spectrum on the CCD array is no more aligned with the CCD lines.
02-JUL2003	GOPR 5.4d	• The maximum number of measurements is set to 509 (instead of 510) in the GOPR prototype.
17-MAR-2003	GOPR 5.4c	• Modification of the CAL ADFs (update of the limb radiometric LUT). The products are affected only if the limb spectra are converted into physical units • Modifications to allow compatibility with ACRI computational cluster (no modifications of the results) • Modification of the logic to handle dark charge map refresh at orbit level (DSA data is now directly processed by the level 1b processor if available in the level 0 product). No impact on the results
21-FEB-2003	GOPR 5.4b	• DC map values are rounded when written in the level 1b product • Modification of the CAL ADFs (update of the wavelength assignment of SPB1 and SPB2) • Modify the computation of flag_mod in the modulation correction routine
17-JAN-2003	GOPR 5.4a	• use the start and stop dates of the occultation when calling the CFI interpol instead of start and stop dates of the level 0 product • modify the ECMWF filename information in the SPH of the level 1b and limb products

5.1.2 AUXILIARY DATA FILES (ADF)

The ADF's files in tables 5.1-3, 5.1-4, 5.1-5, 5.1-6 and 5.1-7 have been disseminated to the PDS during the whole mission. For every type of file, the validity runs from the start validity time until the start validity time of the following one, but if an ADF file has been disseminated after the start validity time, it is obvious that it will be used by the PDS only after the dissemination time (this happens the majority of the times). As the other ADF's, the calibration auxiliary file (GOM_CAL_AX) has been updated several times in the past (table 5.1-7) but the difference is that now it is updated in a weekly basis with only new DC maps, and that is why the files used in December are reported in a separate table (table 5.1-8) that will change from month to month. On 10th and 17th December new calibration ADF's were disseminated with updated DC maps of orbits 09273 and 09380 respectively (table 5.1-8).

The files outlined in yellow are the set of auxiliary files used during the month of December.

Table 5.1-3: Table of historic GOM_PR1_AX files used by PDS for level 1b products generation

Used by PDS for Level 1b products generation in period	GOM_PR1_AX (GOMOS processing level 1b configuration file)
01-MAR-2002 → 29-MAR-2002	GOM_PR1_AXVIEC20020121_165314_20020101_000000_20200101_000000 • Pre-launch configuration
30-MAR-2002 → 14-NOV-2002	GOM_PR1_AXVIEC20020329_115921_20020324_200000_20100101_000000 • Changed num_grid_upper, thr_conv and max_iter in the atmospheric GADS
Not used	GOM_PR1_AXVIEC20020729_083756_20020301_000000_20100101_000000 • Cosmic Ray mode + threshold • DC correction based on maps • Non-linearity correction disabled
Not used	GOM_PR1_AXVIEC20021112_170331_20020301_000000_20100101_000000 • Central background estimation by linear interpolation + associated thresholds
15-NOV-2002 → 26-MAR-2003	GOM_PR1_AXVIEC20021114_153119_20020324_000000_20100101_000000 • Same content as GOM_PR1_AXVIEC20021112_170331_20020301_000000_20100101_000000 but validity start updated so as to supersede according to the PDS file selection rules GOM_PR1_AXVIEC20020329_115921_20020324_200000_20100101_000000
27-MAR-2003	GOM_PR1_AXVIEC20030326_085805_20020324_200000_20100101_000000 • Same content as GOM_PR1_AXVIEC20021112_170331_20020301_000000_20100101_000000 but validity start updated so as to supersede according to the PDS file selection rules GOM_PR1_AXVIEC20020329_115921_20020324_200000_20100101_000000

Table 5.1-4: Table of historic GOM_INS_AX files used by PDS for level 1b products generation

Used by PDS for Level 1b products generation in period	GOM_INS_AX (GOMOS instrument characteristics file)
01-MAR-2002 → 29-JUL-2002	GOM_INS_AXVIEC20020121_165107_20020101_000000_20200101_000000 • Pre-launch configuration
30-JUL-2002 → 12-NOV-2002	GOM_INS_AXVIEC20020729_083625_20020301_000000_20100101_000000 • Factors for the conversion of the SFA angles from SFM axes to GOMOS axes
13-NOV-2002 → 16-JUL-2003	GOM_INS_AXVIEC20021112_170146_20020301_000000_20100101_000000 • No more invalid spectral range
Not used	GOM_INS_AXVIEC20030716_080112_20030711_120000_20100101_000000 • New value for SFM elevation zero offset for redundant chain: 10004
17-JUL-2003	GOM_INS_AXVIEC20030716_105425_20030716_120000_20100101_000000 • Bias induct azimuth redundant value set to -0.0084 rad (-0.4813 deg)

Table 5.1-5: Table of historic GOM_CAT_AX files used by PDS for level 1b products generation

Used by PDS for Level 1b products generation in period	GOM_CAT_AX (GOMOS Star Catalogue file)
01-MAR-2002	GOM_CAT_AXVIEC20020121_161009_20020101_000000_20200101_000000 • Pre-launch configuration

Table 5.1-6: Table of historic GOM_STS_AX files used by PDS for level 1b products generation

Used by PDS for Level 1b products generation in period	GOM_STS_AX (GOMOS Star Spectra file)
01-MAR-2002	GOM_STS_AXVIEC20020121_165822_20020101_000000_20200101_000000 • Pre-launch configuration

Table 5.1-7: Table of historic GOM_CAL_AX files used by PDS for level 1b products generation

Used by PDS for Level 1b products generation in period	GOM_CAL_AX (GOMOS Calibration file)
01-MAR-2002 → 29-JUL-2002	GOM_CAL_AXVIEC20020121_164808_20020101_000000_20200101_000000 • Pre-launch configuration
Not used	GOM_CAL_AXVIEC20020121_142519_20020101_000000_20200101_000000 • Pre-launch configuration
30-JUL-2002 → 12-NOV-2002	GOM_CAL_AXVIEC20020729_082426_20020717_193500_20100101_000000 • Band setting information • Wavelength assignment • Spectral dispersion LUT • ADC offset for Spectrometers • PRNU maps • Thermistor coding LUT • DC maps
Not used	GOM_CAL_AXVIEC20021112_165603_20020914_000000_20100101_000000 • Band setting information

	• DC maps • PRNU maps • Wavelength assignment • Spectral dispersion LUT • Radiometric sensitivity LUT (star and limb) • SP-FP intercalibration LUT • Vignetting LUT • Reflectivity LUT • ADC offset
13-NOV-2002 → 30-JAN-2003	GOM_CAL_AXVIEC20021112_165948_20021019_000000_20100101_000000 • Only DC maps updated
31-JAN-2003 → 11-APR-2003	GOM_CAL_AXVIEC20030130_133032_20030101_000000_20100101_000000 • Only DC maps updated (using DSA of orbit 04541)
12-APR-2003 → 02-JUN-2003	GOM_CAL_AXVIEC20030411_065739_20030407_000000_20100101_000000 • Modification of the radiometric sensitivity curve for the limb spectra. Note that the modification of this LUT has no impact on the GOMOS processing. The LUT is just copied into the level 1b limb product for user conversion purpose. • Updated DC map only (using DSA of orbit 05762).
03-JUN-2003: from this date onwards, only updates to DC maps are done. Every month, the table of new GOM_CAL files with only DC maps updated is provided (table 5.1-8)	GOM_CAL_AXVIEC20030602_094748_20030531_000000_20100101_000000 • Updated DC maps only (using DSA of orbit 06530)

Table 5.1-8: Calibration ADF for December 2003. These files are updated (only with DC maps) in an 8-10 days basis

Used by PDS for Level 1b products generation in period	GOM_CAL_AX (GOMOS Calibration file)
25-NOV-2003 → 07-DEC-2003	GOM_CAL_AXVIEC20031124_155405_20031121_000000_20100101_000000 (orbit 09050, 23-NOV-2003)
08-DEC-2003 → 14-DEC-2003	GOM_CAL_AXVIEC20031210_135039_20031207_000000_20100101_000000 (orbit 09273, 08-DEC-2003)
15-DEC-2003 → 12-JAN-2004	GOM_CAL_AXVIEC20031217_111232_20031214_000000_20100101_000000 (orbit 09380, 16-DEC-2003)

5.2 Quality Flags Monitoring

In this section it is monitored some Product Quality information stored in the level 1b products that are not flagged (MPH error flag not set). The products flagged are around 1.2% of the products received for the quality monitoring.

On the one hand, for every product we have information of the **number of measurements** where a given problem was detected (i.e. number of invalid measurements, number of measurements containing saturated samples, number of measurements with demodulation flag set…). On the other hand, there are **flags** that indicate problems within the product (i.e. flag set to one if the reference spectrum was computed from DB, flag set to zero if SATU data were not used…).

For the information on the number of measurements a plot (percentages) is provided in fig. 5.2-1. It can be seen that the cosmic rays hits occurred often for the 95% of the measurements of the product. Another

observation that can be done is that, for many products, the 30 % of the measurements have the star signal falling outside the central band. The other values (% of invalid measurements per product, % of measurements per product with datation errors…) are quite low.

The flag information is given in table 5.2-1. It is reported also the percentage of the products that have at least one measurement with demodulation flag set.

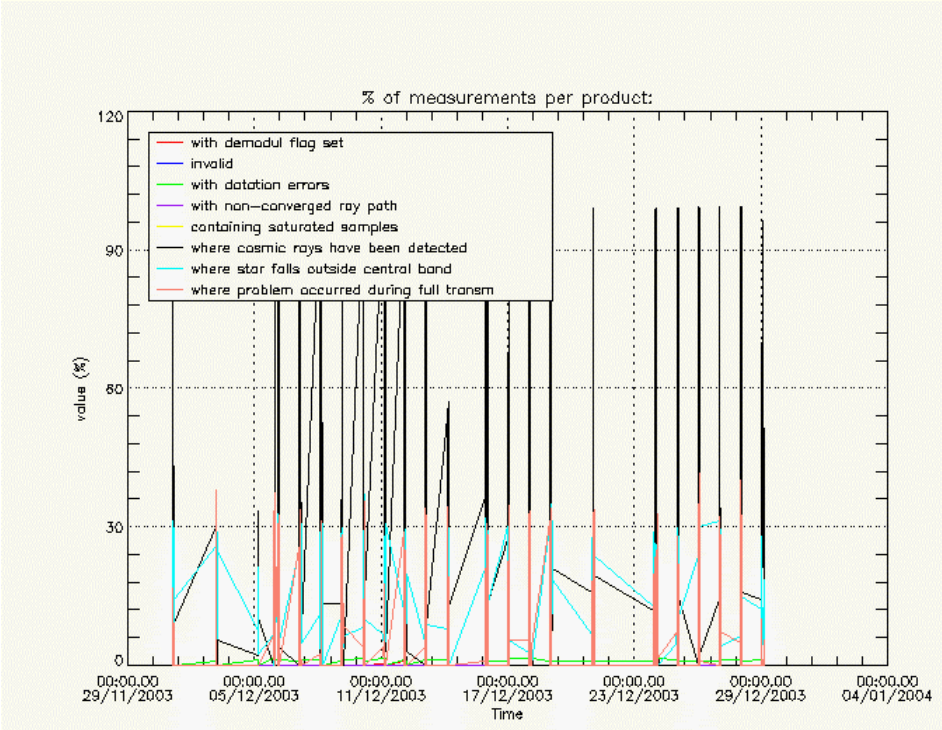

Figure 5.2-1: Level 1b product quality monitoring

At least one measurement with demodulation flag set:	21.0300 %
Reference spectrum computed from DB:	0.00000 %
Reference spectrum with small number of measurements:	0.00000 %
SATU data not used:	0.00000 %

5.3 Spectral Performance

No new spectral calibration has been done during December. These results were already presented in previous versions of the MR with nominal results thus far.

The values reported (table 5.3-1) are, for every star ID (1, 2, 4, 9, 18, 25), the wavelength of the first useful pixel of SPA2. This value is calculated by addition to the actual wavelength assignment, the spectral shift for which a maximum correlation has been found between the reference spectrum and the one of the occultation. It can be observed in table 5.3-1 that for all the stars (but for star id 4) the difference between the actual wavelength (690.492981 nm) and the one reported in the table is between –

0.06 and 0.05 nm. Thus, the wavelength has not been updated in the Calibration product. It is foreseen not to use the star id 4 for wavelength calibration purposes.

Table 5.3-1: Wavelength assignment calculated for several occultations since November 2002

Star ID / Level 0 date	1	2	4	9	18	25
20021112_062935	Occ.30: 690.455750	Occ.26: 690.458740		Occ.28: 690.492981		
20021219_102754		Occ.33: 690.468140	Occ.26: 690.875122			
20030101_151630	Occ.3: 690.445068	Occ.37: 690.466003	Occ.30: 690.878540			
20030110_121504		Occ.32: 690.465088	Occ.25: 690.882385			
20030201_090221						Occ.21: 690.492981
20030415_123156			Occ.29: 690.959534		Occ.20: 690.552002	Occ.28: 690.492981
20030419_170041			Occ.29: 690.957520		Occ.23: 690.555420	
20030428_072600					Occ.19: 690.553645	Occ.28: 690. 492981
20030717_053233				Occ. 22: 690.473816	Occ. 26: 690.446594	

5.4 Radiometric Performance

5.4.1 RADIOMETRIC SENSITIVITY

The monitoring performed consists in the calculation of the radiometric sensitivity of each CCD by computing the ratio between parts of the reference spectrum using specific stars. The parts of spectrum used are:

- UV: 250–300 nm
- Yellow: 500–550 nm
- Red: 640–690 nm
- Ir1: 761-770 nm
- Ir2: 935-944 nm

For the spectrometers the ratios are with respect to the ‘yellow’ spectral range. For the photometers, the ratio is calculated dividing the mean photometer signal above the atmosphere (115 km) by the ‘yellow’ spectral range (for PH1) or by the ‘red’ spectral range (for PH2).

The variation of the normalized ratio should be within a given threshold actually set to 10% (see table 5.4-1 that corresponds to fig. 5.4-1). For every star, this variation is calculated as the difference between the maximum (or minimum) ratio, and the mean over the 15 first values (if there are not 15 values computed yet, all values are used). Values outside the warning threshold of 10% are now observed for the

photometers, and investigations are on going at ACRI ESL. The star 18 has been studied in depth and two possible causes of these abnormal ratios are in place:

- The pointing azimuth of star 18 is going into the vignetting area during the period of the high peak, so the reference star spectrum used for the computation of the radiometric sensitivity ratio contains a contribution due to the vignetting correction. By looking at the UV and Red ratios of fig. 5.4-1, there is no high variation of the ratio, as the vignetting effect does not affect the SPA. For the IR1 and IR2 ratios the high variation seems to be due to some residual error in the vignetting correction.

- Fig. 5.4-2 shows the difference between the SPA reference star spectra for orbits 08010 (azimuth 17.5 deg) and orbit 08428 (azimuth -9 deg). The shape does not look like a star or the sun spectrum; it rather looks like the reflectivity correction curve. It is known that the reflectivity LUT has to be revised and the ESL is currently working on it.

Whether the vignetting or inaccurate reflectivity correction LUT are responsible for the ratios behavior (maybe both) will be checked in the following months, when there will be an updated of the calibration ADF containing a new reflectivity correction LUT.

Table 5.4-1: Variation of RS for the different ratios. Should be less than 10%

Star Id	% Variation of UV ratio	% Variation of Red ratio	% Variation of IR1 ratio	% Variation of IR2 ratio	% Variation of Ph1 ratio	% Variation of Ph2 ratio
1	0.543863	0.207967	0.387800	0.193903	4.16760	10.4636
2	0.158766	0.259793	0.418974	0.216532	3.17917	6.07233
4	0.106818	0.182182	1.17073	1.01013	3.02021	20.1837
9	1.69204	0.213861	0.364793	0.233455	4.79555	9.05862
18	0.223948	0.167108	0.844914	0.608099	14.7885	299.989
25	2.55773	0.212821	0.225987	0.223921	15.9214	78.6219

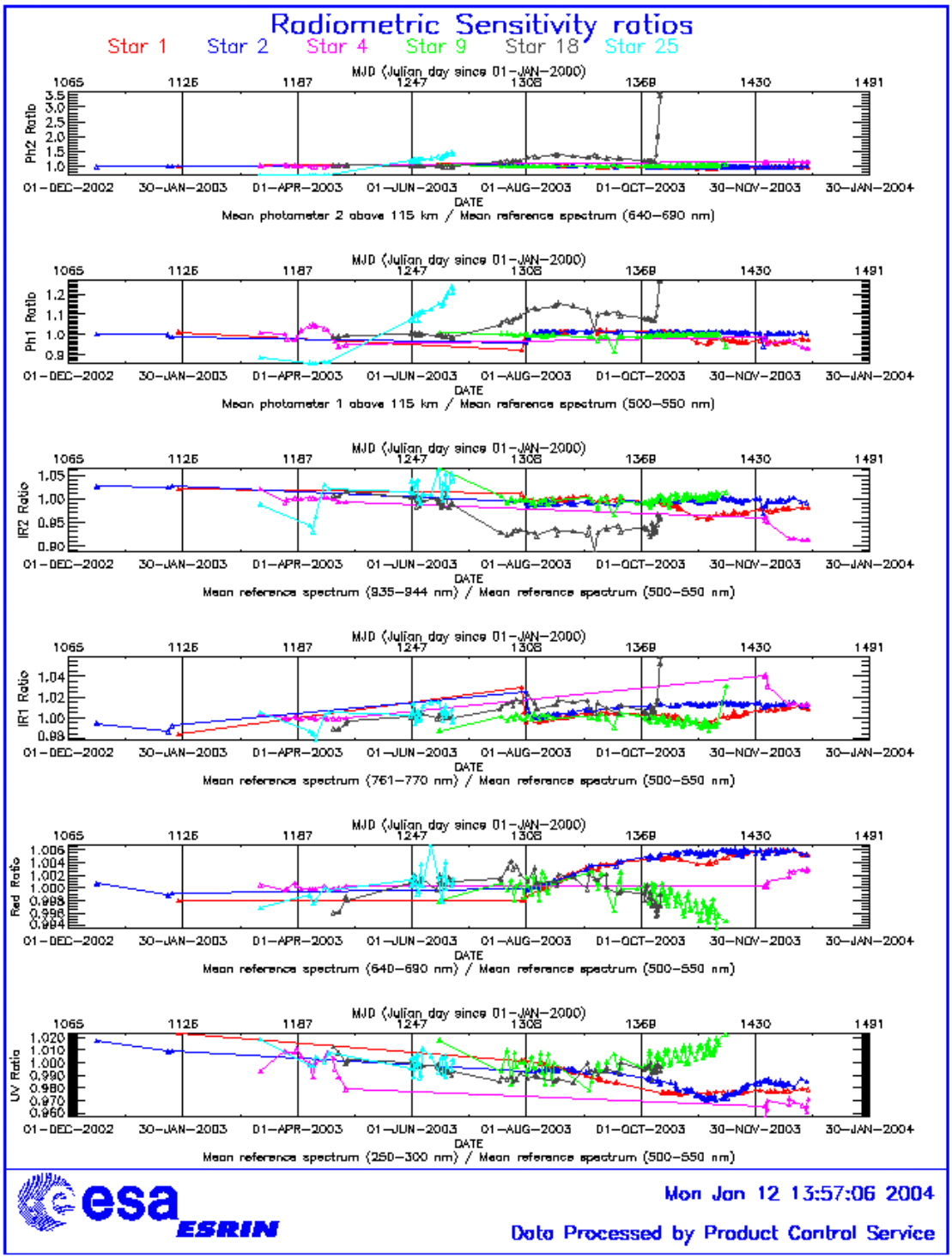

Figure 5.4-1: Radiometric sensitivity ratios

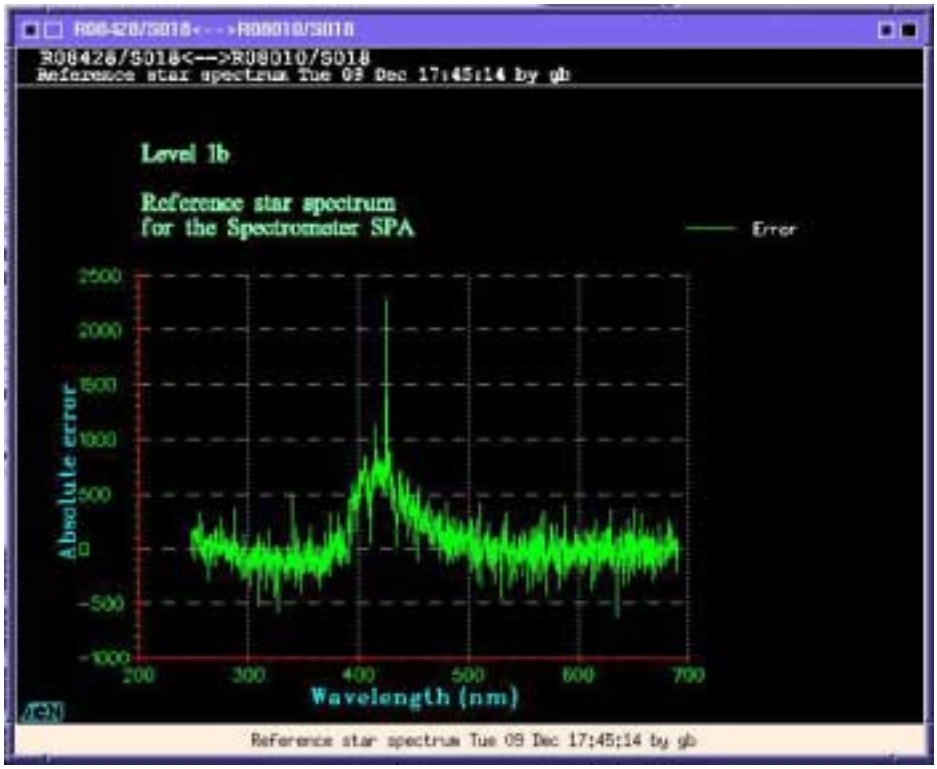

Figure 5.4-2: Difference between the SPA reference star spectra for orbits 08010 (azimuth 17.5 deg) and orbit 08428 (azimuth -9 deg)

5.4.2 PIXEL RESPONSE NON UNIFORMITY

No new PRNU calibration has been done during December. During May 2003 a new PRNU calibration has been performed and processed into an update of the PRNU maps for the SPB1 and SPB2 that have been included in the auxiliary file GOM_CAL disseminated at the end of June 2003.

5.5 Other Calibration Results

Future reports will address other calibration results, when available.

6 LEVEL 2 PRODUCT QUALITY MONITORING

6.1 Processor Configuration

6.1.1 VERSION

No level 2 products from the operational ground segment have been disseminated during December to the users. About 86% of GOM_NL__2P products have been received in the PCF for routine quality control and long term trend monitoring. The current level 2-processor software version for the operational ground

segment is GOMOS/4.00 (see table 6.1-1) and the product specification is PO-RS-MDA-GS2009_10_3H. The improvements defined at the Validation Workshop are currently being implemented into the prototype processor, before implementation into the operational one. In the mean time, Cal/Val teams are supplied with selected data sets generated by the previous prototype processor GOPR 5.4 (see table 6.1-2).

Table 6.1-1: PDS level 2 product version and main modifications implemented

Date	Version	Description of changes
31-MAY-2003	Level 2 version 4.00 at PDHS-E and PDHS-K	Algorithm baseline level 2 DPM 5.4: • Revision of some default values • Add a new parameter • Transmission model computation: suppress tests on valid pixels and species • Apply a Gaussian filter to the vertical inversion matrix • Very low signal values are substituted by threshold value • See ref. [3] for more details
21-NOV-2002	Level 2 version 3.61 at PDHS-E and PDHS-K	Algorithm baseline level 2 DPM 5.3a: • Revision of some default values • Wording of test T11 • Dilution term computation of jend • Covariance computation scaling applied before and after • See ref. [3] for more details

Table 6.1-2: GOPR level 2 product version and main modifications implemented

Date	Version	Description of changes
18-AUG-2003	GOPR 5.4d	• Tikhonov regularisation is implemented
18-MAR-2003	GOPR 5.4b	• Modification to implement the computation of Tmodel for spectrometer B (in version 5.4b, the Tmodel for SPB is still set to 1)
30-JAN-2003	GOPR 5.4a	• Modifications for ACRI internal use only. No impact on level 2 products.

6.1.2 AUXILIARY DATA FILES (ADF)

The ADF's files in table 6.1-3 and 6.1-4 are used by the PDS to process the data from level 1 to level 2. For every type of file, the validity runs from the start validity time until the start validity time of the following one, but if an ADF file has been disseminated after the start validity time, it is obvious that it will be used by the PDS only after the dissemination time (this happens the majority of the times).

Table 6.1-3: Table of historic GOM_PR2_AX files used by PDS for level 2 products generation

Used by PDS for Level 2 products generation in period	GOM_PR2_AX (GOMOS Processing level 2 configuration file)
01-MAR-2002 → 29-JUL-2002	GOM_PR2_AXVIEC20020121_165624_20020101_000000_20200101_000000 • Pre-launch configuration
30-JUL-2002 → 02-SEP-2002	GOM_PR2_AXVIEC20020729_083851_20020301_000000_20100101_000000 • Maximum value of chi2 before a warning flag is raised (set to 5) • Maximum number of iterations for the main loop (set to 1)
03-SEP-2002 → 12-NOV-2003	GOM_PR2_AXVIEC20020902_151029_20020301_000000_20100101_000000 • Maximum value of chi2 before a warning flag is raised (set to 100)
13-NOV-2003	GOM_PR2_AXVIEC20021112_170458_20020301_000000_20100101_000000 • Smoothing mode • Hanning filter • Number of iterations • Spectral windows to suppress the O2 absorption in the high spectral range of SPA2

Table 6.1-4: Table of historic GOM_CRS_AX files used by PDS for level 2 products generation

Used by PDS for Level 2 products generation in period	GOM_CRS_AX (GOMOS Cross Sections file)
01-MAR-2002 → 08-MAR-2002	GOM_CRS_AXVIEC20020121_164026_20020101_000000_20200101_000000 • Pre-launch configuration
09-MAR-2003 → 29-JUL-2002	GOM_CRS_AXVIEC20020308_185417_20020101_000000_20200101_000000 • Corrected NUM_DSD in MPH - was 14 and is now 19 - and corrected spare DSD format by replacing last spare by carriage returns in file GOM_CRS_AXVIEC20020121_164026_20020101_000000_20200101_000000
30-JUL-2002	GOM_CRS_AXVIEC20020729_082931_20020301_000000_20100101_000000 • O3 cross-sections summary description (SPA) • NO3 cross-sections summary description • O2 transmissions summary description • H2O transmissions summary description • O3 cross sections (SPA)

6.2 Other Level 2 Performance Issues

The plot presented in fig. 6.2-1 is the average of the Ozone values during December in a grid of 0.5 degrees in latitude per 1 km in altitude. Some characteristics can be seen as the increase of ozone layer thickness at around 20-25 km at high latitudes due to the transport of O_3 rich air masses. However, other characteristics seem not to be realistic (and are under investigation) as the values below 15 km, where data are not reliable at the moment.

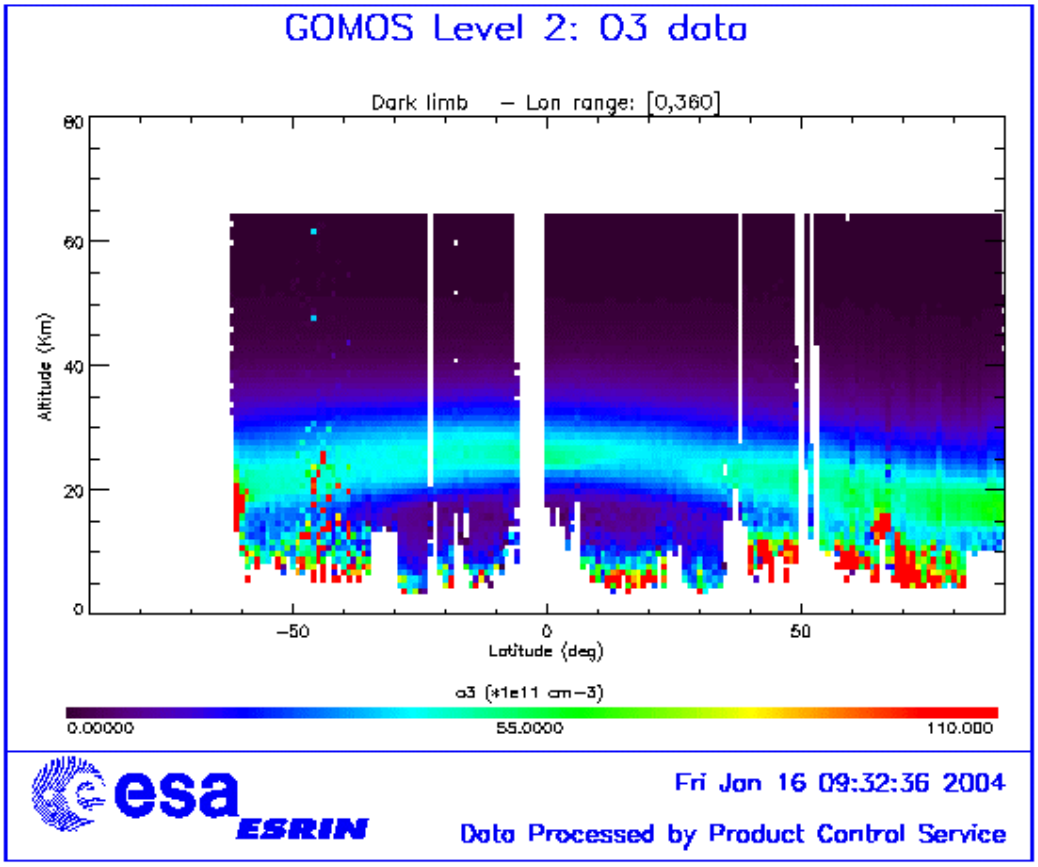

Figure 6.2-1: Average GOMOS O_3 profile during December: average in a grid of 0.5° latitude x 1 km altitude

7 VALIDATION ACTIVITIES AND RESULTS

7.1 Inter-comparison with External Data

7.1.1 COMPARISON WITH LIDAR MEASUREMENTS AT LAUDER (45°S, 169.7°E)

The fig. 7.1-1 plots the vertical profiles of the mean and median difference between the O_3 profiles inferred from GOMOS measurements and measured by the lidar instrument at Lauder. Nineteen lidar profiles were measured during the autumn 2003 at Lauder, and 15 coincidences were found between the GOMOS and the lidar profiles. Gomos profiles are considered in coincidence with lidar measurements if located within 1000 km of Lauder and measured within 4h of the date of lidar measurements. The median profile of the difference highlights negative values below 25km, positive values between 25km and 40km, and negative values above 40km.

Lidar data are courtesy of Daan Swart (RIVM) and were downloaded from the CALVAL NILU database.

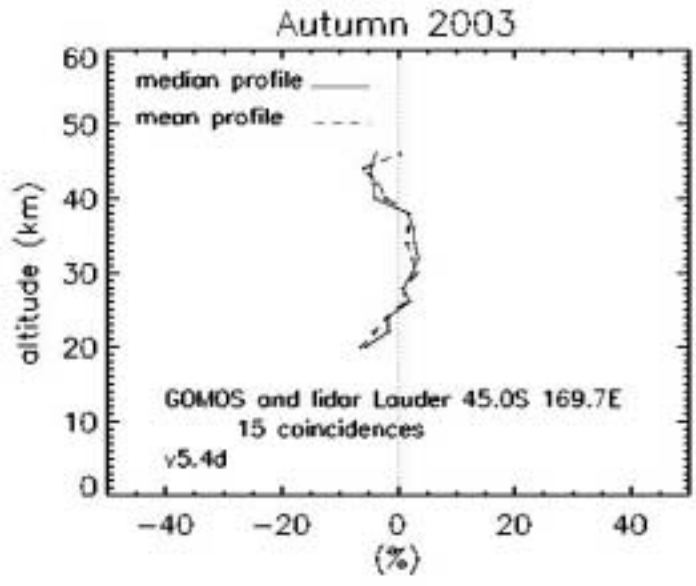

Figure 7.1-1: median and mean vertical profiles of the difference between GOMOS and lidar measurements in coincidence (distance lower than 1000 km and time interval less than 4h)

7.1.2 COMPARISON WITH TOMS MEASUREMENTS

Fig. 7.1-2 shows the correlation between O_3 total values inferred from GOMOS measurements and TOMS O_3 total measurements. Only GOMOS vertical profiles with bottom level higher than 15 km were considered, and about 2800 values inferred from GOMOS measurements were compared to the TOMS measurements. The corresponding Fortuin-Kelder contribution was added to the bottom part of each GOMOS profile in order to be compared to the TOMS measurements. The correlation between the two datasets is quite good, with a coefficient equal to 0.87.

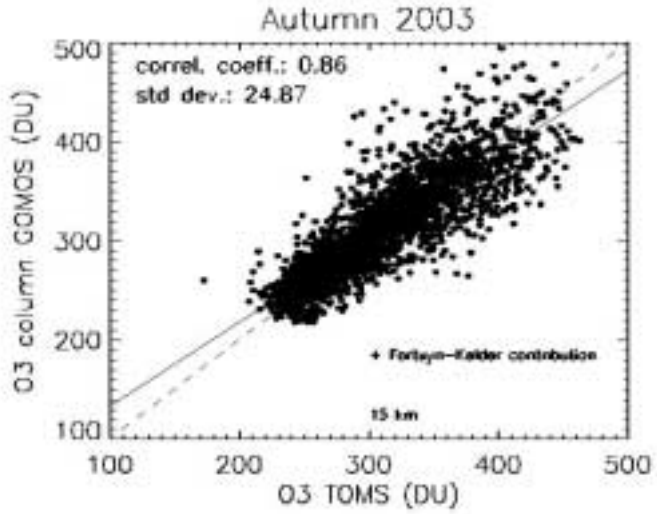

Figure 7.1-2: O_3 column values inferred from GOMOS vertical profiles vs O_3 TOMS values for the corresponding date and location of each GOMOS measurement. Only GOMOS O_3 vertical profiles with bottom altitudes higher than 15 km are considered. The corresponding Fortuin-Kelder contribution is added in the missing part of each profile. The solid line plots the linear fit to the datasets

7.2 GOMOS-Climatology Comparisons

Fig. 7.2-1, 7.2-2, 7.2-3 and 7.2-4 present the percentage difference between GOMOS O_3 values and Fortuyn-Kelder climatology O_3 values as a function of the date of each GOMOS profile, at several pressure levels and within four 10°-width latitude bands. The flagged O_3 values and the O_3 values for which χ^2 are higher than 4 are ruled out of the calculations. Only O_3 profiles inferred from dark occultations have been considered here.

The dispersion of the difference values at level 0.3 hPa in 45°S-35°S is very high compared to other levels. Whereas previous studies for other periods and other versions of L2 data showed that the dispersion of the values at this upper level along with the level 1hPa was generally very high compared to lower levels, it is not the case here for latitude bands other than 45°S-35°S band. At 5hPa, 3hPa and 1hPa, the variability of the difference is lower at low latitudes than at mid-latitudes, and this feature was already stressed out by previous studies.

The difference (GOMOS-climatology) is mostly positive in the upper stratosphere (it is less obvious at 45°N-55°N for levels other than 0.3hPa). This is chiefly due to the use of dark occultations only and to the diurnal variation of ozone in this altitude range.

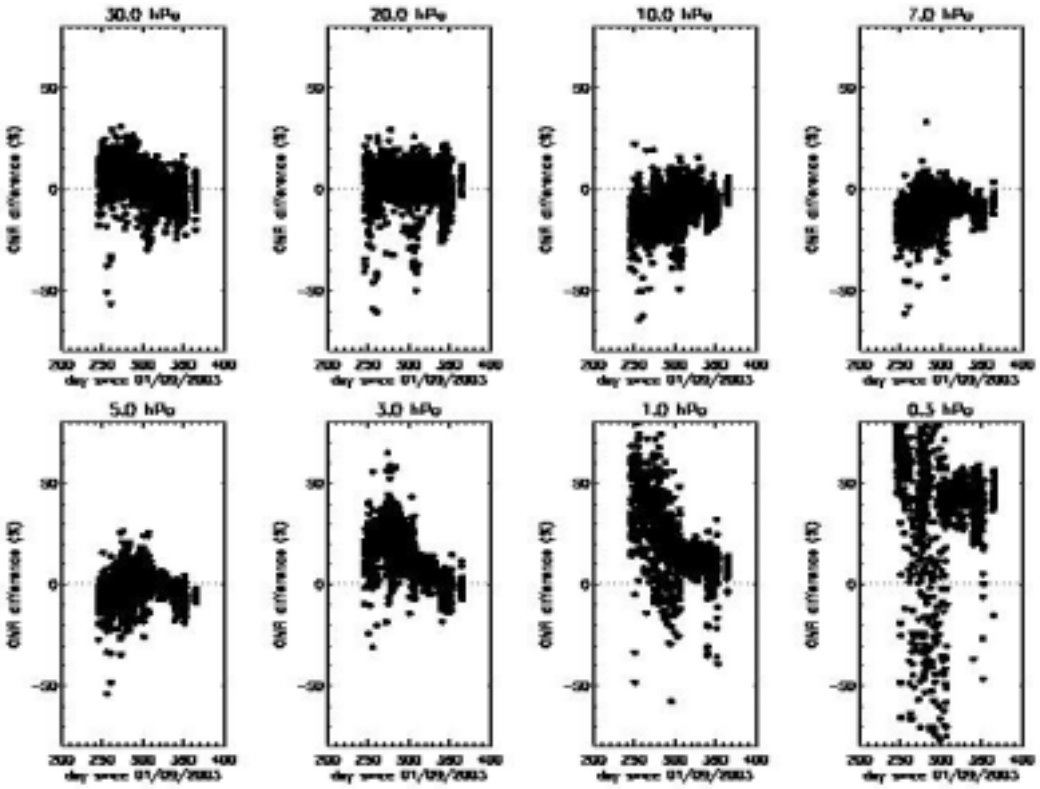

Figure 7.2-1: 45°S-35°S; percentage difference between GOMOS and Fortuin-Kelder climatological values at eight pressure levels and for latitudes between 45°S and 35°S. The difference is plotted as a function of the date of the GOMOS profile

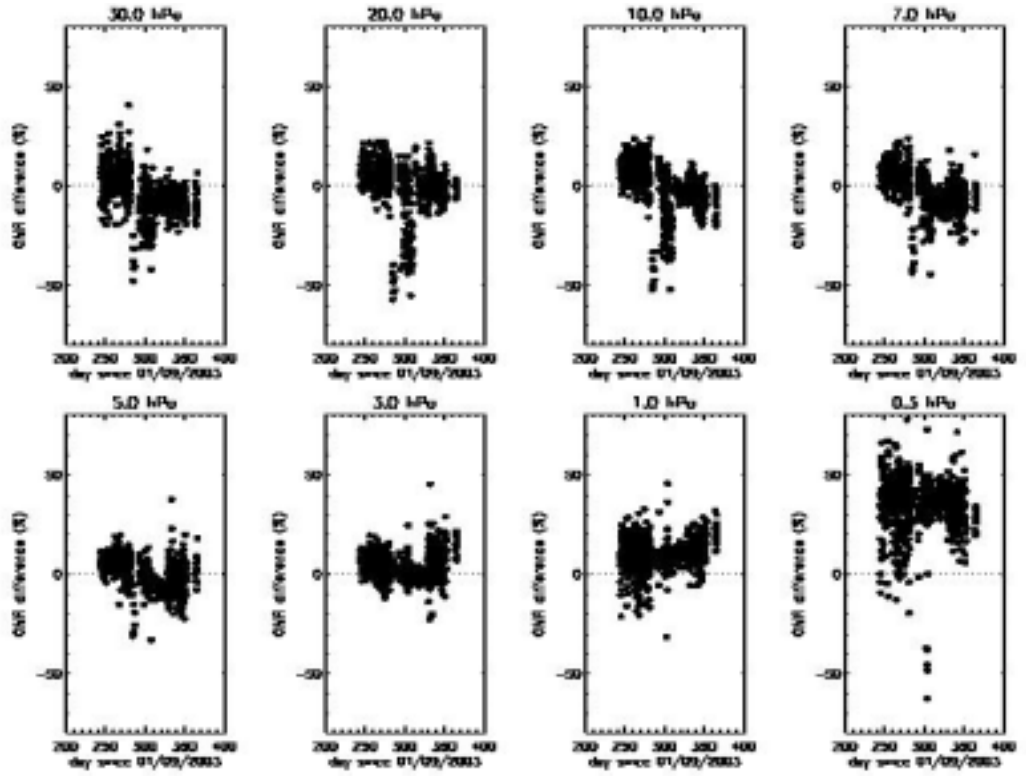

Figure 7.2-2: 5°N-15°N; same as for fig. 7.2-1

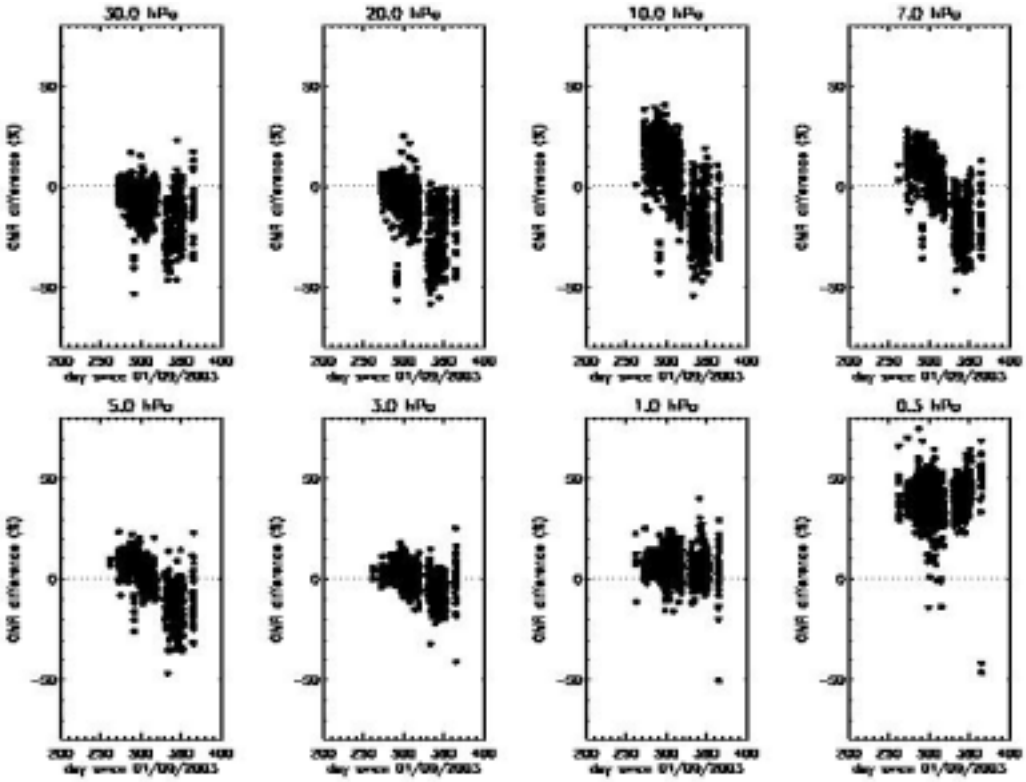

Figure 7.2-3: 25°N-35°N; same as for fig. 7.2-1

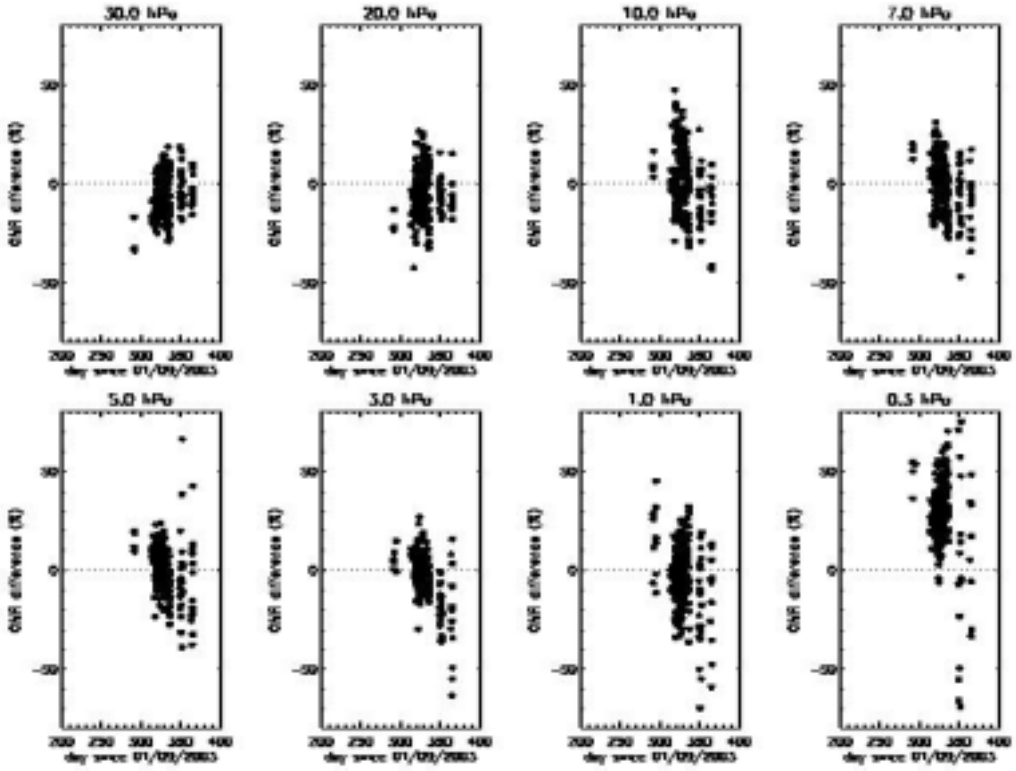

Figure 7.2-4: 45°N-55°N; same as for fig. 7.2-1

7.3 GOMOS Assimilation

Results will be presented upon availability.

7.4 Consistency Verification: GOMOS-GOMOS Inter-comparison

7.4.1 STATISTICAL EVALUATION OF THE PERFORMANCE OF THE GDI (GLOBAL DOAS ITERATIVE) SPECTRAL INVERSION

The goal of this study is to evaluate the impact on line density mean value of NO_2, NO_3 and O_3 and dispersion of NO_2, NO_3 and O_3, aerosols and air when the GDI (Global DOAS Iterative) spectral inversion is applied instead of the global inversion that is currently used in the operational version. The impact of the activation or suppression of some corrections has also been assessed.

The series of 553 S029 occultations from orbit 3960 to orbit 5094 have been used for this study. Five cases have been processed:

1. Global inversion nominal case
2. GDI (Global DOAS Iterative) inversion for NO_2 and NO_3
3. With Air has been forced to ECMWF
4. Global inversion with chromatic refraction correction on

5. GDI inversion with scintillation correction off

Fig. 7.4-1, 7.4-2 and 7.4-3 show the rms dispersion of line density profiles for 5 series of 200 orbits (4000-4199 to 4800-4999), with azimuth angle from 10° to <1° respectively for NO_2, NO_3 and O_3.

- NO_2: a strong decrease of dispersion is observed between 20 and 40 to 50 km depending on the azimuth.
- NO_3: a medium decrease is observed between 35 and 45 km, except for vertical occultations. Some increase may be observed between 30 and 35 km.
- O_3: is slightly affected in both directions.

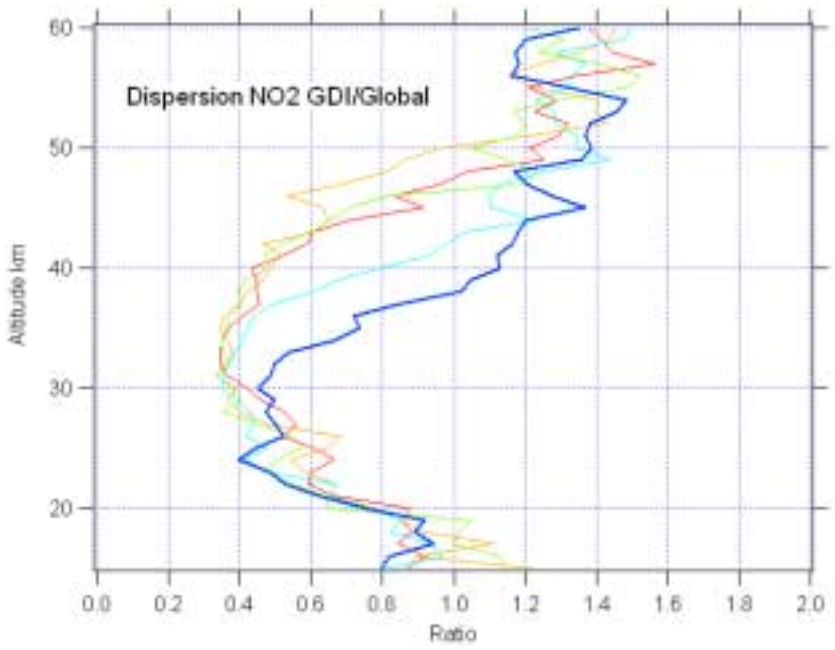

Figure 7.4-1: Mean rms dispersion of NO2 line densities for 5 series of 200 orbits (4000-4199 in red to 4800-4999 in dark blue): ratio between GDI and global spectral inversion

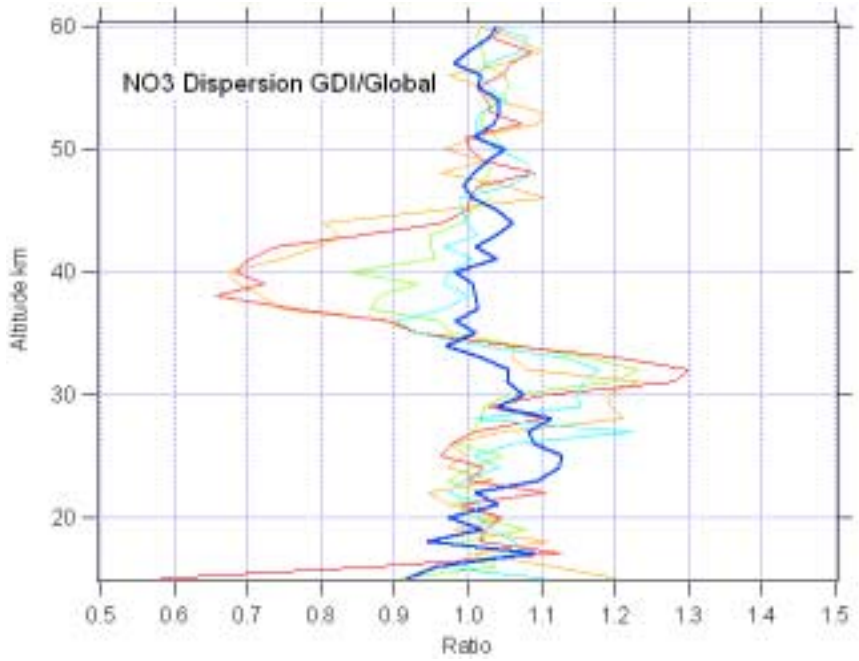

Figure 7.4-2: Mean rms dispersion of NO3 line densities for 5 series of 200 orbits (4000-4199 in red to 4800-4999 in dark blue) ratio between GDI and global spectral inversion

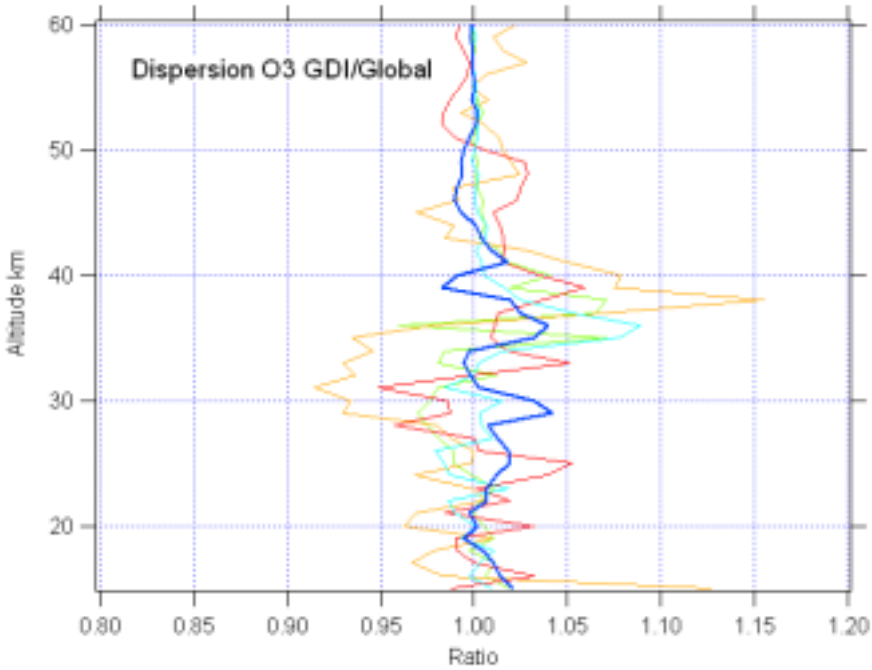

Figure 7.4-3: Mean rms dispersion of O3 line densities for 5 series of 200 orbits (4000-4199 in red to 4800-4999 in dark blue): ratio between GDI and global spectral inversion

Fig. 7.4-4, 7.4-5 and 7.4-6 show the rms dispersion of NO_2, NO_3 and O_3 in the series 4400-4599 in different cases. It can be seen that:

- The refraction correction has a small impact
- When air is forced by ECMWF the dispersion is in general increased.
- The suppression of scintillation correction has a small impact.

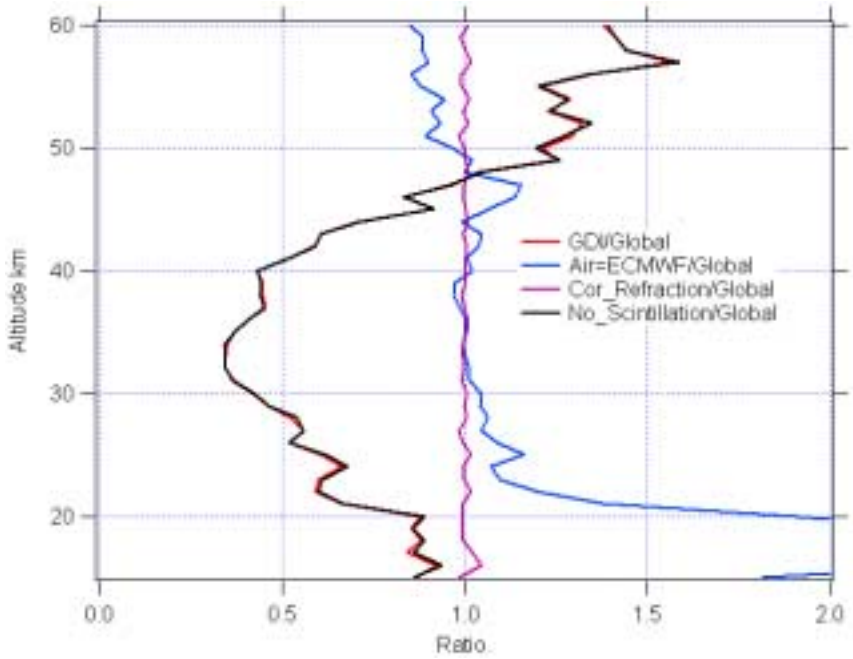

Figure 7.4-4: Mean rms dispersion of NO_2 line densities 200 orbits (4400-4599): ratio with global inversion in several cases

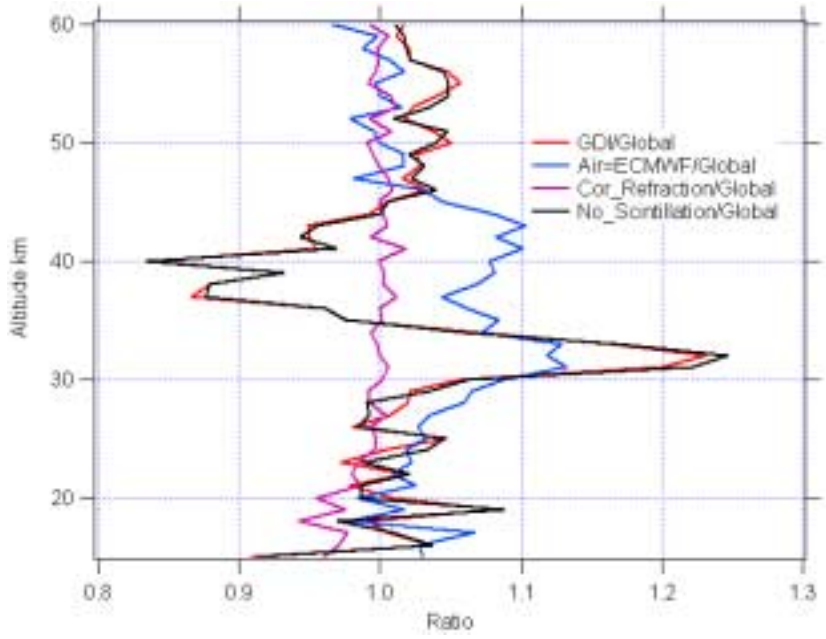

Figure 7.4-5: Mean rms dispersion of NO_3 line densities 200 orbits (4400-4599): ratio with global inversion in several cases (see text)

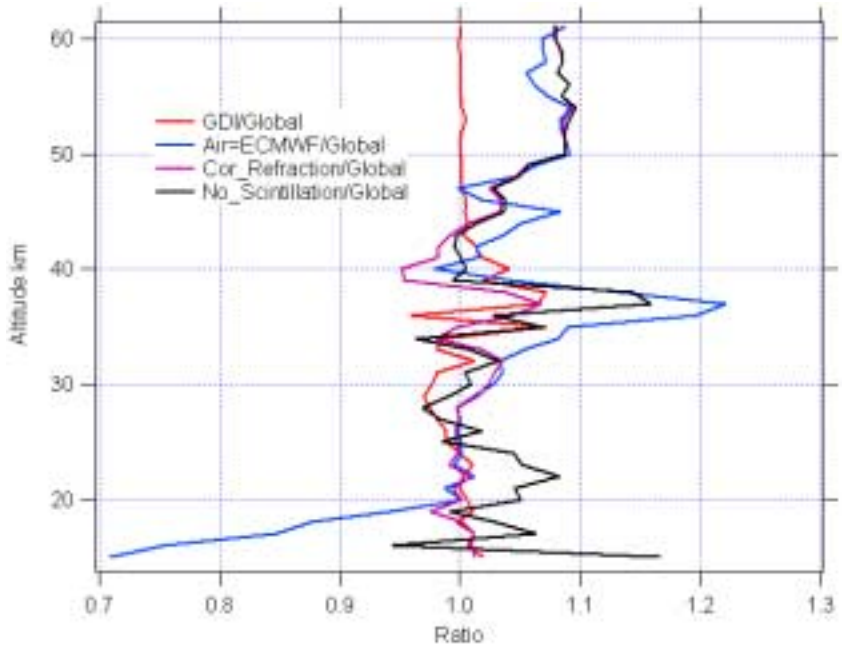

Figure 7.4-6: Mean rms dispersion of O_3 line densities 200 orbits (4400-4599): ratio with global inversion in several cases (see text)

Fig. 7.4-7, 7.4-8 to 7.4-9 show the GDI to Global ratio between the mean profile of NO_2, NO_3 and O_3 for each series of 200 orbits.

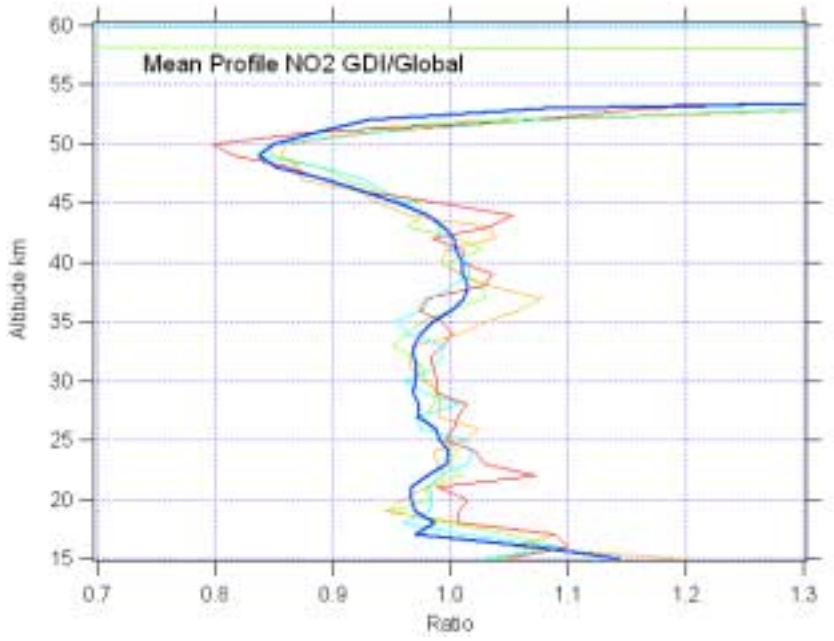

Figure 7.4-7: mean NO_2 line density profile: ratio between GDI and Global for the 5 200-orbit-series

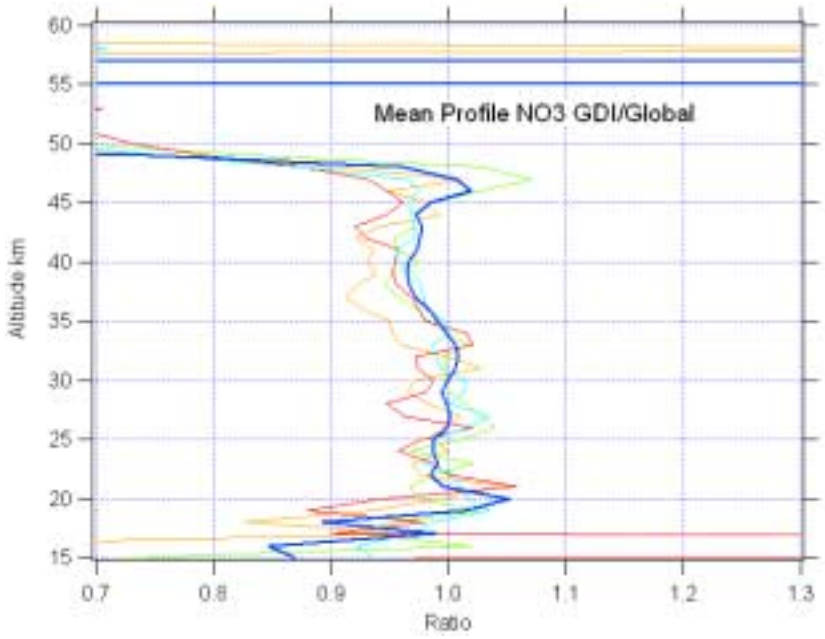

Figure 7.4-8: mean NO_3 line density profile: ratio between GDI and Global for the 5 200-orbit-series

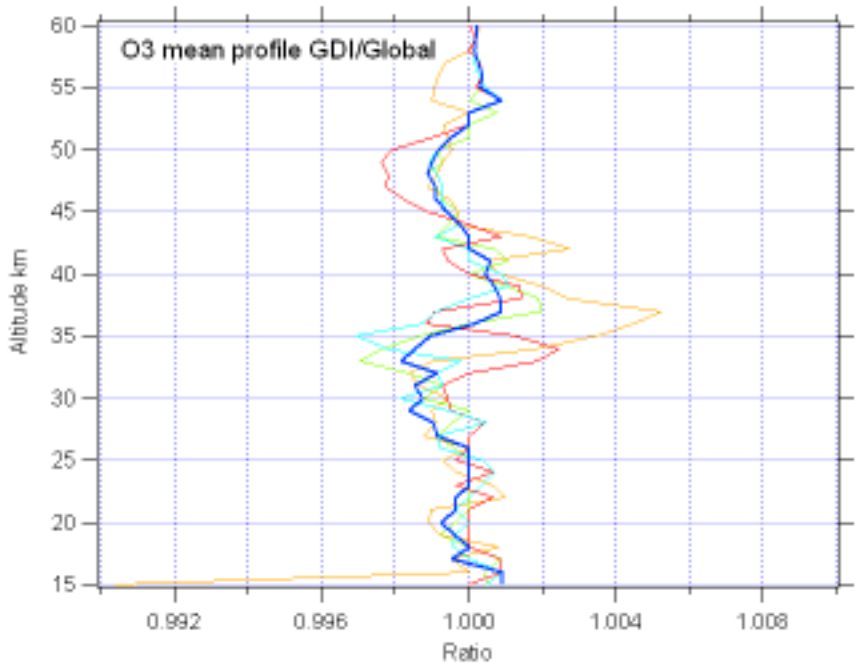

Figure 7.4-9: mean O3 line density profile: ratio between GDI and Global for the 5 200-orbit-series

- NO_2: the ratio is between 0.95 and 1.08 in the altitude range 20-45 km. The deviation from 1 is larger above and below but error bars are very large.
- NO_3: the ratio is between 0.92 and 1.06 in the altitude range 20-45 km. The deviation from 1 is larger above and below but error bars are very large.

- O_3: the ratio remains very near 1, between 0.997 and 1.005 between 16 and 60 km. It means that GDI for NO_2 and NO_3 does not perturb O_3.

Fig. 7.4-10, and 7.4-11 present the impact of GDI and the scintillation correction on the dispersion of air and aerosols for occultations measured between orbits 4400 and 4599. The vertical profile of the dispersion of air and aerosols is plotted for three cases:

1. Global processing
2. GDI
3. GDI with no correction of scintillation

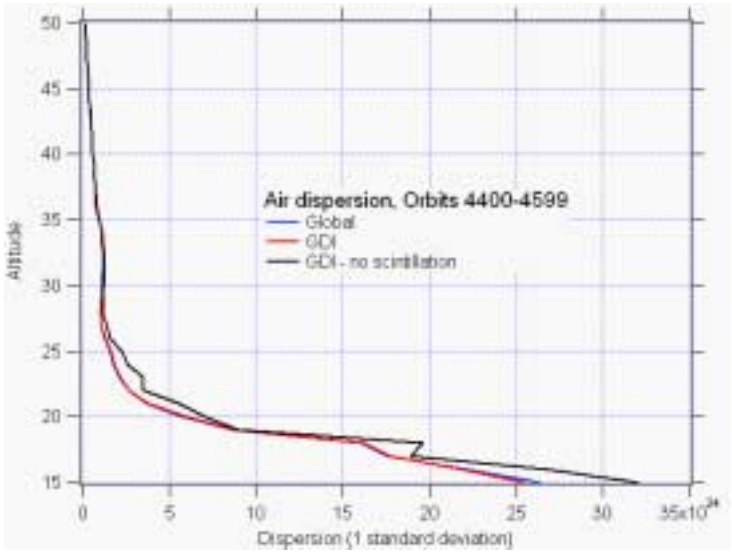

Figure 7.4-10: Vertical profile of the air dispersion for orbits 4400-4599, for three processing cases

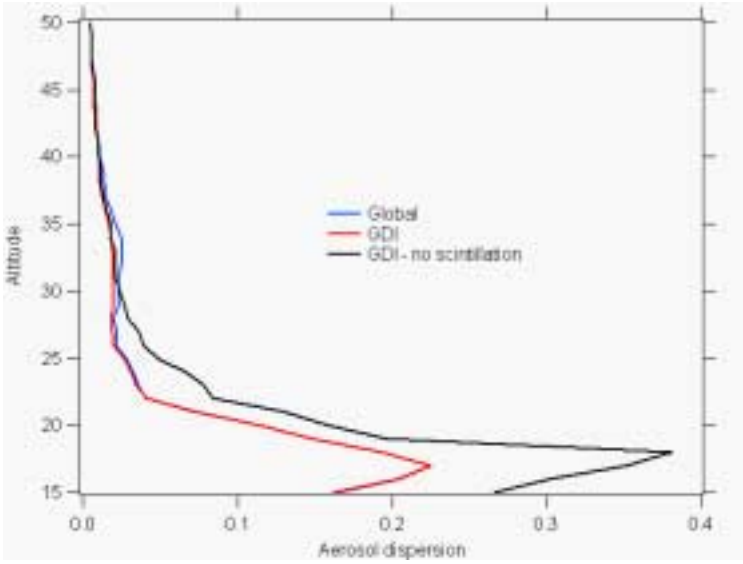

Figure 7.4-11: Vertical profile of the aerosol dispersion for orbits between 4400-4599, for three processing cases

Some conclusions can be extracted:

- GOMOS ozone profiles show very good agreement when compared with external validated data sources, using the Tikhonov regularisation. Activating GDI for NO2 and NO3 shows no degradation of ozone retrieval.
- GDI should be activated for NO_2 below 38 km (for a vertical occultation) and below 50 km for an oblique occultation. The expected gain is a factor 2 to 3 in the standard deviation between 25 and about 40 km.
- Activation of GDI would improve data products for NO3 between 35 and 45 km for oblique occultations. The expected gain is up to 30% in standard deviation around 40 km.
- Activation of GDI would improve the dispersion of aerosols, lowered between 25km and 40km (by more than 20% between 30km and 35km). Very small or no effect is observed on the air dispersion.
- The main effect of the scintillation correction is a significant decrease of the dispersion of the aerosols, and a smaller decrease of the air dispersion below 32km. The scintillation correction has a small (positive) impact on the dispersion of the other species line densities. Scintillation correction must therefore be applied, as it is in the current nominal processing chain
- When air is forced to ECMWF, an increase of the other species line density dispersion is observed. Inversion of air should therefore be maintained, as it is in the current nominal processing chain.
- The chromatic refraction correction has a small impact on the dispersion of line densities. It could be activated in the nominal chain, however it has to be first checked that it does not introduce any numerical instabilities when processing a wider dataset.